

# The Geomechanics of CO<sub>2</sub> Storage in Deep Sedimentary Formations

Jonny Rutqvist

Received: 8 September 2011 / Accepted: 30 December 2011 / Published online: 12 January 2012  
© The Author(s) 2012. This article is published with open access at Springerlink.com

**Abstract** This paper provides a review of the geomechanics and modeling of geomechanics associated with geologic carbon storage (GCS), focusing on storage in deep sedimentary formations, in particular saline aquifers. The paper first introduces the concept of storage in deep sedimentary formations, the geomechanical processes and issues related with such an operation, and the relevant geomechanical modeling tools. This is followed by a more detailed review of geomechanical aspects, including reservoir stress-strain and microseismicity, well integrity, caprock sealing performance, and the potential for fault reactivation and notable (felt) seismic events. Geomechanical observations at current GCS field deployments, mainly at the In Salah CO<sub>2</sub> storage project in Algeria, are also integrated into the review. The In Salah project, with its injection into a relatively thin, low-permeability sandstone is an excellent analogue to the saline aquifers that might be used for large scale GCS in parts of Northwest Europe, the U.S. Midwest, and China. Some of the lessons learned at In Salah related to geomechanics are discussed, including how monitoring of geomechanical responses is used for detecting subsurface geomechanical changes and tracking fluid movements, and how such monitoring and geomechanical analyses have led to preventative

changes in the injection parameters. Recently, the importance of geomechanics has become more widely recognized among GCS stakeholders, especially with respect to the potential for triggering notable (felt) seismic events and how such events could impact the long-term integrity of a CO<sub>2</sub> repository (as well as how it could impact the public perception of GCS). As described in the paper, to date, no notable seismic event has been reported from any of the current CO<sub>2</sub> storage projects, although some unfelt microseismic activities have been detected by geophones. However, potential future commercial GCS operations from large power plants will require injection at a much larger scale. For such large-scale injections, a staged, learn-as-you-go approach is recommended, involving a gradual increase of injection rates combined with continuous monitoring of geomechanical changes, as well as siting beneath a multiple layered overburden for multiple flow barrier protection, should an unexpected deep fault reactivation occur.

**Keywords** CO<sub>2</sub> storage · Geomechanics · Caprock · Fault reactivation · Seismicity · Modeling · Saline formations

## 1 Introduction

A growing concern that increasing levels of greenhouse gases in the atmosphere are contributing to

---

J. Rutqvist (✉)  
Lawrence Berkeley National Laboratory (LBNL),  
Berkeley, CA 94720, USA  
e-mail: jrutqvist@lbl.gov

global climate change has led to a search for economical and environmentally sound ways to reduce carbon dioxide (CO<sub>2</sub>) emissions. One promising approach is CO<sub>2</sub> capture and storage (CCS) in deep geologic formations, such as depleted oil and gas reservoirs, unminable coal seams, and deep saline aquifers (Bachu 2008; Benson and Cole 2008; Bickle 2009; Plasynski et al. 2011). Geological media suitable for CO<sub>2</sub> storage must have sufficient capacity and injectivity, and must confine, or at least sufficiently delay the lateral or vertical migration of CO<sub>2</sub> to the surface. Such geological media are mainly deep sedimentary formations, including oil and gas reservoirs and deep saline aquifers (Bachu 2008; Benson and Cole 2008; Bickle 2009).

Recent experience from CO<sub>2</sub> injection at a number of pilot projects, as well as a few ongoing commercial projects demonstrates that CO<sub>2</sub> geological storage in deep sedimentary formations is technologically feasible (Michael et al. 2010). However, if CCS is implemented on the scale needed to make noticeable reductions in atmospheric CO<sub>2</sub>, a billion metric tons or more must be stored annually, with the largest injection operations in regions with the highest CO<sub>2</sub> emissions (Benson and Cole 2008). Securing such a large volume will require a solid scientific foundation, and that defines the coupled hydrologic–geochemical–geomechanical processes that govern the long-term fate of CO<sub>2</sub> in the subsurface. Also needed are methods to characterize and select sequestration sites, subsurface engineering to optimize performance and cost, approaches for ensuring safe operation, monitoring technology, remediation methods, regulatory overview, and an institutional approach for managing long-term liability (Benson and Cole 2008).

Geomechanical processes associated with geologic carbon storage (GCS) received some initial attention in the late 1990s. A few published generic modeling studies and discussions indicated that geomechanics would likely play a central role should GCS be applied at a large scale (Rutqvist and Tsang 2002; Saripalli and McGrail 2002; Li et al. 2002; Streit and Hillis. 2004; Yamamoto and Takahashi 2004; Hawkes et al. 2005). More recently, studies of actual CO<sub>2</sub> injection sites, such as the In Salah CO<sub>2</sub> storage project in Algeria, have shown that significant geomechanical changes may indeed occur, depending on the injection pressure and site specific geomechanical conditions (e.g. Rutqvist et al. 2010; Bissell et al. 2011; Verdon et al. 2011; Zhou

et al. 2010). The importance of geomechanics has recently become more widely recognized as the possible magnitude and extent of pressure disturbance associated with large-scale CO<sub>2</sub> storage operations have become more apparent (Zoback 2010). There are concerns related to the potential for triggering notable (felt) seismic events and how such events could impact the long-term integrity of a CO<sub>2</sub> repository, as well as how it could impact the public perception of GCS (Zoback 2010). The shut-down of a geothermal project in Basel after a 3.4 magnitude seismic event (Håring et al. 2008) is a recent well-known example, in which ground motion felt by nearby communities was a show stopper. Recently, some GCS projects (e.g., in the Netherlands and Germany) have been put on hold because of public concerns about potential earthquakes, leakage, and impact on property values. Ultimately, it might be public perception that will determine whether CCS is implemented at a large scale (Benson and Cole 2008). Thus, large-scale GCS has to be developed with great care, and geomechanics will play a key role in site-specific GCS risk analyses to ensure safe operation.

This paper provides a review of the geomechanics associated with CO<sub>2</sub> storage in deep sedimentary formations, in particular saline aquifers, the most promising GCS option in terms of storage capacity, but still challenging in terms of site characterization and assessment of containment. The paper first introduces the concept of storage in deep sedimentary formations, the geomechanical processes and issues related to such an operation, and the relevant geomechanical modeling tools. This is followed by a more detailed review of geomechanical aspects, including reservoir stress-strain and microseismicity, well integrity, caprock sealing performance, and the potential for fault reactivation and notable seismic events. Geomechanical observations at some of the current GCS field deployments are also integrated into the review. To date, the most important and outstanding GCS deployment from a geomechanical perspective is the In Salah CO<sub>2</sub> storage project (Mathieson et al. 2010, 2011). At In Salah, CO<sub>2</sub> is injected at about a 1.8–1.9 km depth into a relatively tight and thin sandstone formation at an injection overpressure substantially above initial formation pressure. At this site, injection-induced geomechanical changes have been observed and these are important components of the field monitoring program (Mathieson et al. 2010, 2011). Some geomechanical

changes have also been observed at other CO<sub>2</sub> storage projects, such as Weyburn, Canada (Chalaturnyk 2007; White 2009) and Arnech, Utah (Zhou et al. 2010), which are both associated with enhanced oil recovery (EOR). At the North-Sea-based Sleipner CO<sub>2</sub> storage project, on the other hand, no significant geomechanical changes have been detected, which is not surprising considering the minimal injection overpressure at that site (Eiken et al. 2011). The In Salah CO<sub>2</sub> storage project, with its relatively low-permeability injection zone, is an excellent analogue for deep saline formations in large parts of Northwest Europe, the U.S. Midwest, and China, where large scale GSC will be an attractive option for mitigating CO<sub>2</sub> emissions from large power plants (Wright et al. 2009). Lessons learned from the In Salah project will be particularly important for what we can learn about managing significant geomechanical changes occurring in the field and how such mechanical changes can be utilized for field monitoring and verification of the underground storage performance.

## 2 GCS in Deep Sedimentary Formations

As mentioned, geologic media suitable for GCS consist mainly of oil and gas reservoirs and deep saline aquifers that are found in sedimentary basins (Bachu 2008; Benson and Cole 2008; Bickle 2009). Storage of gases, including CO<sub>2</sub>, in these media has been demonstrated on a commercial scale by past EOR operations, natural gas storage, and acid gas disposal. Some of the risks associated with GCS are similar to these industrial activities for which extensive safety and regulatory frameworks are in place. Specific risks are related to the operational (injection) phase and to the post-operational phase, where the risks of most concern are those posed by the potential for acute or chronic CO<sub>2</sub> leakage from the storage site (Bachu 2008).

Geological media suitable for GCS must have the following characteristics (Bachu 2008):

- Capacity, to accept the intended volume of CO<sub>2</sub>.
- Injectivity, to take in CO<sub>2</sub> at the rate that it is supplied from the CO<sub>2</sub> emitter(s).
- Confinement, to prevent the migration and leakage of the buoyant and mobile CO<sub>2</sub> from the storage space to other places in the subsurface, to shallow potable groundwater or to the surface.

Deep sedimentary formations can possess these characteristics, because generally only sandstone and carbonate rocks have the porosity needed to provide storage capacity and the permeability required for injectivity. At the same time, confining low-permeability shales and evaporites, such as salt beds and anhydrites, provide a primary physical barrier to CO<sub>2</sub> migration out of the intended storage unit (Bachu 2008). In such formations, injection could take place at a depth below 800 m so that the CO<sub>2</sub> would be within the temperature and pressure range for it to be a supercritical fluid. As a supercritical fluid, the CO<sub>2</sub> behaves like a gas with low viscosity, but has a liquid-like density of 200–900 kg/m<sup>3</sup>, depending on pressure and temperature. Thus, large volumes of CO<sub>2</sub> gas would be compressed to a higher density supercritical fluid, and stored in a much smaller volume.

In deep sedimentary formations, CO<sub>2</sub> can be stored through a variety of physical and chemical trapping mechanisms (Gunter et al. 2004; Bachu 2008; Benson and Cole 2008). Physical trapping includes: (1) static trapping of mobile CO<sub>2</sub> in stratigraphic and structural traps, as well as (2) residual-gas trapping in the pore space at irreducible gas saturation, in which case CO<sub>2</sub> is immobile because of the interfacial tension between CO<sub>2</sub> and formation water. Chemical trapping occurs when CO<sub>2</sub> dissolves in subsurface fluids (solubility and ionic trapping) and may then be involved in chemical reactions with the rock matrix (mineral trapping). The CO<sub>2</sub> will first be trapped by primary mechanisms, namely static and hydrodynamic trapping below the caprock in oil and gas reservoirs and deep saline aquifers. Over time, a series of secondary (chemical) trapping mechanisms start operating, mechanisms that do not necessarily increase the CO<sub>2</sub> storage capacity, but do increase the storage security (i.e., diminish the potential for leakage and the amount of CO<sub>2</sub> that may migrate or leak) (IPCC 2005; Bachu 2008; Benson and Cole 2008). As will be discussed below, while geomechanics is important both for the short and long-term performance of a CO<sub>2</sub> repository, it is perhaps most important related to physical trapping during active CO<sub>2</sub> injection.

## 3 Geomechanical Processes and Key Technical Issues

Figure 1 presents an overview of geomechanical processes and key technical issues that will be

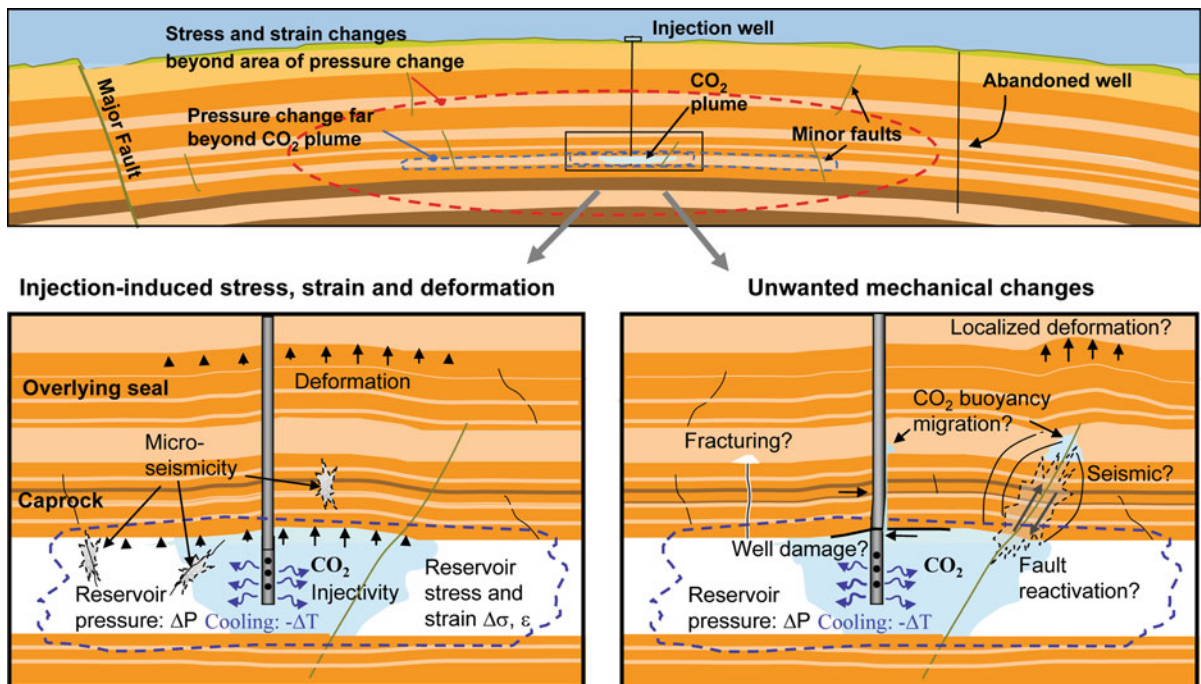


**Fig. 1** Geomechanical processes and key technical issues associated with GCS in deep sedimentary formations. *Top* the different regions of influence for a CO<sub>2</sub> plume, reservoir pressure changes, and geomechanical changes in a multilayered system with minor and major faults. *Bottom left* injection-

induced stress, strain, deformations and potential microseismic events as a result of changes in reservoir pressure and temperature, and *bottom right* unwanted inelastic changes that might reduce sequestration efficiency and cause concerns in the local community

discussed in detail in the following sections of this paper. The top figure illustrates that geomechanical changes occur far beyond the area of actual pressure changes, which in turn extends far beyond the CO<sub>2</sub> plume. Any change (even small) in reservoir pressure and temperature will induce some stress-and-strain changes in and around the injection zone (Fig. 1, bottom left). This may result in detectable ground-surface deformations and could also lead to noticeable changes in permeability and injectivity. Moreover, the injection-induced fluid pressure and straining of the reservoir and surrounding rock may result in small seismic events that could be detected by geophones. Such microseismic events can be triggered under the right circumstances, depending on factors such as *in situ* stress, injection pressure, existence and nature of fractures, and rock properties. Even a small pressure change and straining of the rock might result in small microseismic events because of rock heterogeneities, including fractures and local stress concentrations that could be released locally. As will be further discussed, these types of geomechanical responses, including

ground-surface uplift and microseismic events, have been observed at CO<sub>2</sub> storage sites as well as in other types of underground injection operations, and are generally useful for monitoring of subsurface fluid flow and geomechanical processes (Mathieson et al. 2011; Teatinia et al. 2011; Burch et al. 2009).

If reservoir pressure becomes sufficiently high, more substantial, irreversible mechanical changes could occur, e.g., creating new fractures, straining the well assembly, or reactivating larger faults within the reservoir, in the caprock or overburden (Fig. 1, bottom right). This could possibly open new flow paths through otherwise low-permeability capping formations and thereby enable enhanced, buoyancy-driven, upward migration of the injected CO<sub>2</sub>. Moreover, reactivation of a fault could potentially result in a notable seismic event (e.g. magnitude >3) that, if felt, may raise concern in local communities. Notable seismic events might also be induced by reactivating minor faults (e.g., faults a few hundred meters long) that might intersect the injection zone but might not be detectable by seismic surveys. For this reason, a

multilayered system of several low permeability layers in the overburden (as illustrated in Fig. 1, top) will be important for impeding upward migration of the CO<sub>2</sub>, even in the event of fault reactivation at the depth of the injection zone.

Considering these geomechanical processes and key technical issues, it is obvious that geomechanics plays a central role in determining the suitability of an injection site, including the potential for triggering notable seismic events and other risks. A risk assessment will be required at any future commercial GCS site and might be performed at the early stages of a project to help in site selection, communicating project goals and procedures to the public, and aiding regulators in permitting for the project (Stauffer et al. 2009; Oldenburg et al. 2009). In such a risk analysis, key technical risk features, events, and processes related to geomechanics is not limited to notable seismic events; but also include the risk for CO<sub>2</sub> release to shallow potable-groundwater aquifers or to the surface, e.g., via leaky wells or faults.

#### 4 Coupled Flow and Geomechanical Models for GCS

In recent years, a number of coupled fluid flow and geomechanical numerical models have emerged as suitable for the analyzing various geomechanical issues associated with GCS. Desirable capabilities for such a numerical simulator include the capture of non-isothermal multiphase flow and transport for supercritical CO<sub>2</sub> and brine coupled with geomechanical processes. Examples of the numerical simulators applied to study the geomechanical aspects of GCS, include TOUGH-FLAC (Rutqvist et al. 2002; Rutqvist 2011), FEMH (Bower and Zyvoloski 1997; Deng et al. 2011), OpenGeoSys (Wang and Kolditz 2007; Goerke et al. 2011), CODE-BRIGHT (Olivella et al. 1994; Vilarrasaa et al. 2010), ECLIPSE-VISAGE (Ouellet et al. 2011), STARS (CMG 2003; Bissell et al. 2011), NUFT-SYNEF (Morris et al. 2011a, b), DYNFLOW (Preisig and Prévost 2011), as well as other simulators in which multiphase flow codes such as TOUGH2, ECLIPSE, and GEM have been linked with geomechanical codes (e.g. Rohmer and Seyedi 2010; Ferronato et al. 2010; Tran et al. 2010). Some coupled fluid flow and geomechanical simulators can also include geochemistry of various levels of sophistication, from

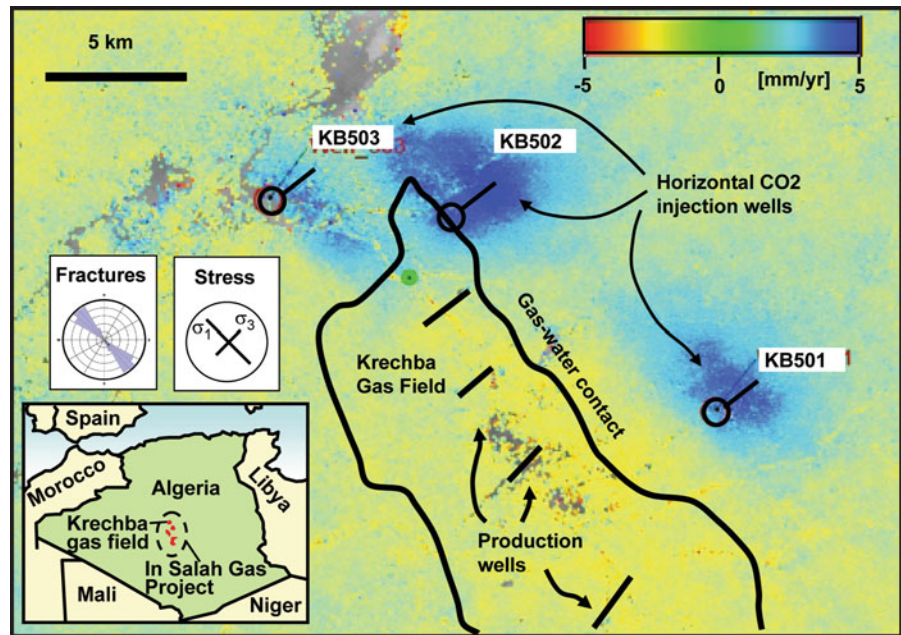
nonreactive to fully reactive solute transport, e.g., linking TOUGHREACT to FLAC<sup>3D</sup> (Rutqvist et al. 2002; Taron et al. 2009), or Retraso to CodeBright (Kvamme and Liu 2009). Such capabilities can be used to assess long-term geochemical and geomechanical changes in reservoir and caprock when exposed to CO<sub>2</sub>. These coupled models require a large number of input parameters that might not be readily available, such as parameters for geomechanical-geochemical interactions. In fact, simplified models might be sufficient for studying subsets of coupled processes. For example, when studying large-scale geomechanical changes and the potential for fault reactivation, driven by large-scale reservoir pressure changes, a single phase fluid flow model coupled with geomechanics might be sufficient (e.g. Chiaramonte et al. 2011a). Moreover, analytical and semi-analytical models (e.g. Streit and Hillis 2004; Soltanzadeh and Hawkes 2009; Selvadurai 2009; Mathias et al. 2010; Rohmer and Olivier 2010) or numerical multiphase flow models linked with analytical geomechanical models (e.g. Lucier et al. 2006; Chiaramonte et al. 2008; Vidal-Gilbert et al. 2010) can also be useful for first-order analysis and quick assessment of CO<sub>2</sub> injection-site suitability.

#### 5 Injection-Induced Strain, Stress and Microseismicity

As soon as fluid injection starts, changes in reservoir stresses and strains can quickly propagate laterally within the injection zone, along with an expanding fluid pressure. The pressurization causes vertical expansion of the reservoir and changes in the stress field. These induced changes are, in general, proportional to the magnitude of the pressure increase,  $\Delta P$ , and depend on the geometry and geomechanical properties (such as compressibility) of the reservoir and surrounding sediments.

The vertical expansion of the reservoir may result in a ground surface deformation that might be detectable using state-of-the-art satellite-based interferometry (InSAR) and tilt meters. The magnitude of uplift will also depend on the thickness of the underground reservoir being pressurized at depth. For example, the possibility of CO<sub>2</sub> or water injection into a saline sandy aquifer lying 600–800 m under the lagoon of Venice, Italy, has been suggested for lifting

**Fig. 2** InSAR data for average distance change (close to vertical displacement) evaluated by Tele-Rilevamento Europa (TRE) from August 2004 though March 2007. Fracture orientation rose diagram from Iding and Ringrose (2010), and stress orientations evaluated by Geosciences Ltd, UK (Darling 2006). Cold (green to blue) colors with positive values indicate uplift, whereas hot (green to red) indicate subsidence



Venice from the sea, an estimated 30 cm (Abbot 2004; Comerlati et al. 2006; Castelletto et al. 2008). At the In Salah CO<sub>2</sub> storage project, around 2.5 cm of uplift have been observed as a result of CO<sub>2</sub> injection (Fig. 2). Over the first few years of injection, the InSAR data showed an uplift rate on the order of 5 mm per year above active CO<sub>2</sub> injection wells, with the uplift bulges extending laterally several kilometers from each injection well (Vasco et al. 2008a, b; Mathieson et al. 2009; Rutqvist et al. 2010). One reason for the high resolution of the InSAR data at In Salah is favorable ground-surface conditions, consisting of relatively hard desert sediments and bare rock.

The few centimeters uplift observed above In Salah CO<sub>2</sub> injection wells might seem remarkable, considering that injection takes place into a thin (20 m thick) sandstone formation at a depth of almost 2 km. However, a few-centimeters uplift can actually be estimated using simple analytical calculations. Assuming a thin, laterally extensive reservoir, the uplift can be estimated according to (Fjær et al. 2008):

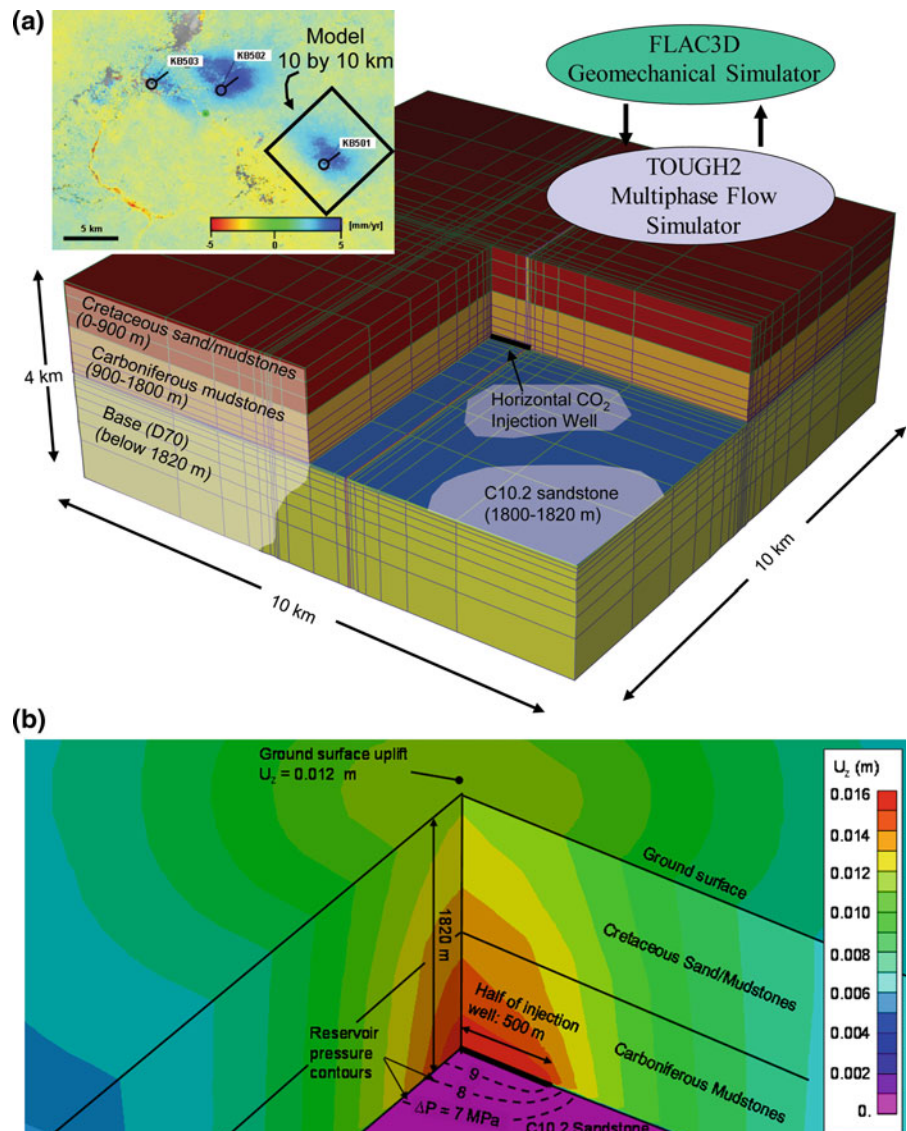
$$\frac{\Delta h}{h} = \alpha \frac{(1 + \nu)(1 - 2\nu)}{(1 - \nu)E} \Delta P \quad (1)$$

where  $\Delta h$  is the vertical expansion of the reservoir,  $h$  is the thickness of the reservoir,  $\alpha$  is Biot's coefficient,  $\nu$  is Poisson's ratio,  $E$  is Young's modulus, and  $\Delta P$  is the change in reservoir pressure. For  $\nu = 0.2$ ,  $E = 6$  GPa,

$h = 20$  m,  $\alpha = 1$ , and  $\Delta P = 10$  MPa (using parameters from Rutqvist et al. 2010), a vertical expansion of 3 cm is possible. The uplift estimated using Eq. 1 is a rough approximation because it assumes that changes in well pressure expand uniformly and laterally over a very large distance; it is a 1-dimensional uplift model that will likely overestimate the uplift, but within the correct order of magnitude. In reality, the uplift will depend on an average pressure within the injection zone, which is lower than the well pressure. Moreover, the stiffness of the overburden rock will result in a bending moment that tends to restrict the vertical expansion of the reservoir. Such effects might be considered by using more complex semi-analytical methods (e.g. Geertsma 1973; Fjær et al. 2008; Selvadurai 2009), or alternatively by using coupled numerical models as described below.

Inverse semi-analytical deformation analysis by Vasco et al. (2008a, b) and coupled numerical modeling by Rutqvist et al. (2010) showed that the observed uplift at the In Salah CO<sub>2</sub>-injection wells could indeed be explained by pressure-induced expansive straining of the rock formations at the depth of the injection, at least for the first few years of injection. Figure 3 shows one example in which the calculated uplift is caused solely by pressure-induced elastic expansion within the 20 m thick injection zone. Figure 3b illustrates that the uplift is caused by

**Fig. 3** TOUGH-FLAC coupled CO<sub>2</sub> injection and geomechanical modeling of ground surface uplift around a horizontal injection well at In Salah. **a** Geometry of model centered around an injection well, and **b** vertical displacement and reservoir fluid pressure around the injector after 3 years of injection (Rutqvist et al. 2011b)



reservoir pressure changes (which are laterally more extensive than the CO<sub>2</sub> plume). It also shows that the uplift is somewhat restricted by the overburden stiffness; the vertical displacement is about 1.6 cm at the top of the injection zone, but attenuated to an uplift of about 1.2 cm of the ground surface (Fig. 3b). The 1.2 cm uplift magnitude was in agreement with observed magnitude at injection well KB-501 after the first 2.5 years of injection. In this case, the combination of the InSAR observations and analysis of the coupled subsurface processes provided a clear indication that the injected CO<sub>2</sub> and displaced brine stayed within the intended storage unit at depths of

about 1.8–1.9 km. More recently, surface uplift data have indicated the opening of a deep fractured zone or fault near the KB-502 well; and this will be further discussed below in Sect. 9.

The stress evolution within and around the reservoir is important as a source of potential mechanical inelastic responses, including shear reactivation of existing fractures that could result in seismic events. During injection, the vertical stress will be approximately constant, equal to the weight of the overburden. The horizontal stress, on the other hand, will change with the injection as a result of poro-elastic stress, a phenomenon commonly observed during oil and gas

production (Zoback 2007). The injection-induced changes in horizontal stress will depend on the geometry and poro-elastic properties of the reservoir-caprock system (Rutqvist et al. 2007, 2008).

We may estimate changes in horizontal stress analytically, again assuming a thin, laterally extensive reservoir (i.e., the so-called passive basin) according to Hawkes et al. (2005):

$$\Delta\sigma_h = \alpha \frac{1-2\nu}{1-\nu} \Delta P \quad (2)$$

In this case, with  $\alpha = 1$  and  $\nu = 0.2$ , applying Eq. 2 gives  $\Delta\sigma_h = 0.75\Delta P$ . That is, the total horizontal stress would increase by a factor of 0.75 of the fluid pressure change. Again, for more complex geometries, alternative semi-analytical methods or coupled numerical models could be used (Rutqvist et al. 2008; Rohmer and Olivier 2010; Soltanzadeh and Hawkes 2009).

In Rutqvist et al. (2011a), numerical simulation results were used for a first order estimate of the potential for injection-induced microseismicity at In Salah. The numerical modeling was used for calculating changes in the effective stress field as a result of the injection, and a Mohr-Coulomb failure criterion was used to evaluate the likelihood of shear slip reactivation along existing fractures (and associated induced microseismicity). At In Salah, fractures within the injection zone are known to be subvertical, most of them striking roughly NW-SE, which is parallel to the direction of the in situ maximum principal stress (Iding and Ringrose 2010). Considering that shear-slip reactivation could take place along subvertical fractures, Rutqvist et al. (2011a) derived

the following simple criterion for the onset of shear slip:

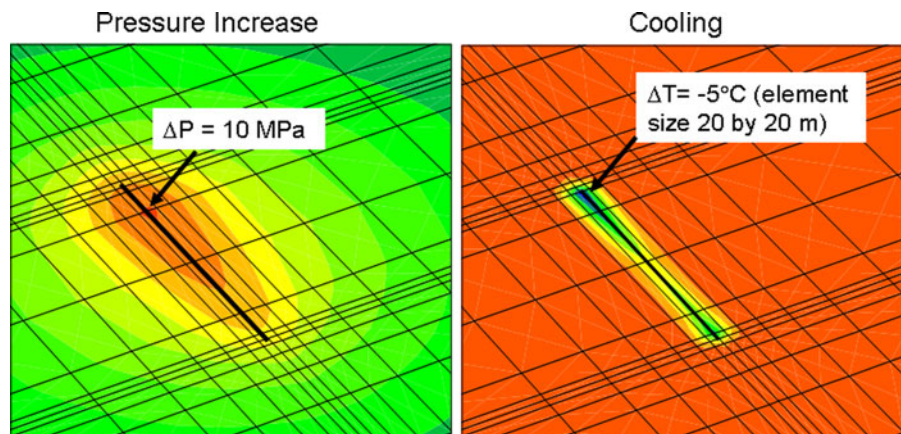
$$\sigma'_H \geq \sigma'_{Hc} = 3\sigma'_h \quad (3)$$

where  $\sigma'_H$  is the maximum compressive horizontal effective stress,  $\sigma'_{Hc}$  is the critical maximum compressive horizontal effective stress for the onset of shear failure, and  $\sigma'_h$  is the minimum compressive horizontal effective stress. The factor 3 in this expression comes from an assumption of cohesionless fractures and faults with a friction angle of  $\phi = 30^\circ$ , which may be considered a lower limit value of frictional strength for fractures in sandstone. The results shown in Figs. 4 and 5 from Rutqvist et al. (2011a) indicated that the highest potential for induced microseismic events would occur near the injection well as a result of the combined effects of injection-induced cooling and pressure increase. The results in Fig. 5 are expressed in terms of a strength-to-stress margin,  $\sigma'_{mc}$ , as

$$\sigma'_{mc} = \sigma'_{Hc} - \sigma'_H = 3\sigma'_h - \sigma'_H \quad (4)$$

The results in Fig. 5 have been updated from that of Rutqvist et al. (2011a), showing a slightly higher potential for microseismic events. For a best estimate of the in situ stress field at the assumed depth in this model simulation (with the injection zone located at 1,800–1,820 m below ground surface), the simulation results showed a negative margin close the wellbore, meaning that calculated shear stress exceeds the shear strength of optimally oriented fractures, which therefore could slip. Consequently, the injection-induced stresses would be sufficient to induce seismicity close to the wellbore. Preliminary microseismic monitoring at the site indicates that some microseismic events

**Fig. 4** Results of coupled nonisothermal, multiphase flow modeling of CO<sub>2</sub> injection showing changes in reservoir fluid pressure and temperature after about 3 years of injection





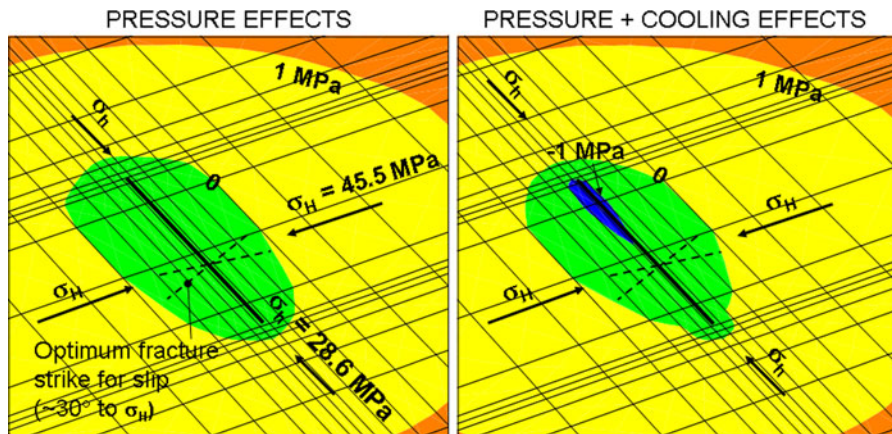


**Fig. 5** Calculated potential for induced seismicity expressed in terms of a strength-to-stress margin after about 3 years of injection. The minimum strength-to-stress margin < 0 close to

the well (blue and green contours) means that the rock-mass stress exceeds the strength, indicating that shear slip and microseismicity could occur in this area

occur and may be correlated with the injection rate. If these events were located, close to one of the injection wells, and if more advanced source and moment tensor analysis can be made, such data can be used to calibrate the geomechanical model and to provide a better understanding of the underground geomechanical processes at the site (Rutqvist et al. 2011a).

Again, a simple analytical analysis may be useful, this time to estimate the potential for induced seismicity and compare with the numerical simulation results. Using the stress magnitudes shown in Fig. 5, and an initial hydrostatic fluid pressure of 18.1 MPa, the strength-to-stress margin before injection can be estimated to  $\sigma'_{mci} = 3\sigma'_h - \sigma'_H = 3(S_h - P_i) - (S_H - P_i) = 3(28.6 - 18.1) - (45.5 - 18.1) = 4.1$  MPa. For a maximum fluid pressure of about 28.1 MPa (or an overpressure  $\Delta P = 10$  MPa), the strength-to-stress margin can be estimated as  $\sigma'_{mc} = 3\sigma'_h - \sigma'_H = 3(S_h + \Delta\sigma_h - P_i - \Delta P) - (S_H + \Delta\sigma_H - P_i - \Delta P) = \sigma'_{mci} + 2(\Delta\sigma_h - \Delta P) = 4.1 + 2(7.5 - 10) = -0.9$  MPa. To this, one can also add an estimate of stress changes caused by the cooling shrinkage of the rock around the wellbore. For the volume around the wellbore at the scale of tens of meters, a maximum cooling of about  $\Delta T = -5^\circ\text{C}$  was calculated from the numerical simulation (Fig. 4). One can then estimate the thermal stress from  $\Delta\sigma_T = \alpha_T \times \Delta T \times E/(1 - 2\nu)$  (assuming a fully constrained sediment) where  $\alpha_T$  is the coefficient of linear thermal expansion. For  $\alpha_T = 1 \times 10^{-5} \text{ }^\circ\text{C}^{-1}$ ,  $\Delta T = -5^\circ\text{C}$ ,  $E = 6$  GPa,  $\nu = 0.2$ , we arrive at a cooling-induced stress of  $-0.5$  MPa. The strength-to-stress margin can then be estimated as  $\sigma'_{mc} = \sigma'_{mci} + 2(\Delta\sigma_p$

$+\Delta\sigma_T - \Delta P) = 4.1 + 2(7.5 - 0.5 - 10) = -1.7$  MPa. This value is consistent with the numerically calculated values close to the injection well in Fig. 5 and therefore provides confidence in the numerically calculated distribution.

Seismic monitoring and analysis associated with CO<sub>2</sub> injection have also been conducted at the Otway project, Australia (Myer and Daley 2011), at Weyburn, Canada (Verdon et al. 2011) and at the Aneth oil field, Utah (Zhou et al. 2010). At Otway, microseismic monitoring indicates a low level of seismicity (typically less than 5 events per day) with magnitudes of less than 0, and no clear correlation with injection pressure history (Myer and Daley 2011). Both Weyburn and Aneth are related to EOR in carbonate reservoirs. At Weyburn, monitoring of induced microseismicity has been conducted since 2003, in a section of the field where injection was initiated in a nearby vertical well in 2004. In total, less than 100 events with magnitudes ranging from  $-1$  to  $-3$  have been recorded, documenting a low rate of seismicity. Many events were located in the overburden outside the injection zone and interpreted to be triggered by stress transfer from injection-induced expansion of the reservoir (Verdon et al. 2011). At Aneth, a large number of microseismic events have been recorded since 2008 at magnitudes ranging from  $-1$  to  $0$ , episodically at rates up to approximately 10 events per day. The events delineate two NW-SE oriented fracture zones located on opposite flanks of the reservoir (Fig. 6). Variations in the microseismic activity in these zones may have been caused by critically stressed structures driven by

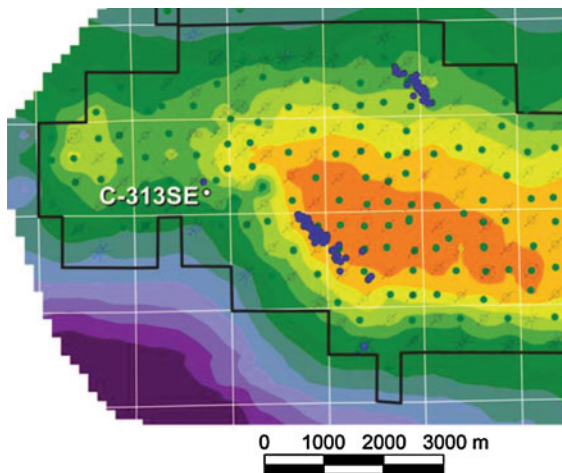


**Fig. 6** Structural contour map of the Aneth reservoir (Utah) showing microseismic event locations (*blue dots*) recorded in a passive seismic array. Southern cluster interpreted to be related to stress-induced fracturing ahead of CO<sub>2</sub> front, northern cluster interpreted as stress induced fault reactivation or stress arching in the overburden (Zhou et al. 2010; Rutledge et al. 2009)

longer-term production- and/or injection-induced stress changes (Zhou et al. 2010).

The observations from both Weyburn and Aneth, illustrate the fact that geomechanical changes can occur outside the injection zone and are not necessarily confined to areas where the actual pressure changes occurs (Rutqvist et al. 2008). Microseismic activities in the overburden have also been observed during reservoir pressure depletion associated with hydrocarbon production at some fields (Segall 1989; Odonne et al. 1999). Note, however that all the injection induced microseismic events recorded at In Salah, Otway, Weyburn and Aneth to date are so small that they are only detectable using geophones. For example, the biggest events of magnitude 0 or less as recorded at Aneth and Otway could be associated with shear slip along fractures with radius on the order of a meter or less. The clustered microseismic activities along structures such as observed at Aneth have also been observed at other underground injection operations, including the 1970s fluid injection experiments at Matsushiro, Japan (Ohtake 1974; Cappa et al. 2009), and Rangeley, Colorado (Raleigh et al. 1976), as well as at the Soultz geothermal project in France (Baisch et al. 2010). This indicates the existence of a fracture network, for example associated with the damage zone around a fault or within fractured rock zones where

smaller (meter scale) fractures can be reactivated or mechanically coalesced. As will be discussed in more detail in Sect. 9, larger events that can be felt would require much larger source dimension. For example, a magnitude 4 seismic event would require a km-sized fault-rupture area (Cappa and Rutqvist 2011b).

Finally, reservoir stress and strain evolution might also be impacted by chemically mediated compaction, especially in carbonate rich reservoirs, where CO<sub>2</sub> exposure would promote dissolution of minerals. It is well known from CO<sub>2</sub> flooding related to EOR that dissolution of carbonates in rock-forming minerals may enhance porosity and permeability, leading to worm holes and fingering (Ross et al. 1982). Moreover, enhanced mineral dissolution may also lead to mechanical weakening as well as enhanced compaction creep and subsidence (Nguyen et al. 2011; Spiers et al. 2010; Le Guen et al. 2007; Espinoza et al. 2011). A number of laboratory studies have investigated the effects of supercritical CO<sub>2</sub> on rock samples, showing the importance of intergranular pressure solution, especially in limestone with rock-forming carbonates, but also in sandstones with cementing carbonates. In general, experiments have shown that CO<sub>2</sub> exposure leads to acceleration of creep by up to several orders of magnitude in carbonate-rich rocks (Le Guen et al. 2007; Spiers et al. 2010). In a field setting, such increased compaction strain will not only impact the stress evolution within the reservoir, but (through stress transfer) the surrounding rock and overburden as well, and lead to some irreversible subsidence. Very few laboratory data exist and no field studies related to CO<sub>2</sub> injection have been focused on the potential for chemically mediated compaction so it is difficult to quantify this effect. Le Guen et al. (2007) observed about 1% compaction strain over a year of exposure to CO<sub>2</sub>-rich fluid and to estimate long term effects such data could perhaps be extrapolated to tens or hundreds of years using mechanical creep models.

## 6 GCS Injectivity and Limits on Injection Pressure

For a site with a given injectivity, the injection rate will be limited by the maximum overpressure that can safely be applied without causing any unwanted damaging geomechanical changes that could jeopardize the confinement of the injected CO<sub>2</sub>. Future

regulations related to underground CO<sub>2</sub> injection might limit the admissible injection pressure to the fracturing gradient evaluated by leak-off tests in the caprock, just above the intended storage zone. For example, it is the current practice for deep injection of liquid waste in the U.S regulatory standard that maximum injection pressure should be less than the measured fracture-closure pressure. Below the fracture-closure pressure, any existing fractures cannot open and no new fractures can form, implying no enhanced migration of waste fluids out of the injection intervals (USEPA 1994). The regional guidance for implementation is that the maximum injection pressure can be determined either by a site-specific fracture-closure pressure derived from direct or indirect testing, or by formation-specific default values for the fracture-closure pressure gradients. For example, a default value of 0.0129 MPa/m (130% of the hydrostatic pressure gradient) is given for the Mt. Simon formation in Illinois; 0.0181 MPa/m (181% of the hydrostatic pressure gradient) is reported for the Dundee Limestone in the Michigan Basin (USEPA 1994; Zhou et al. 2008). In the case of acid gas injections in western Canada, the operating license limits the maximum bottom-hole pressure to no higher than 90% of the fracturing pressure, to ensure that fracturing of the caprock does not occur, but in many cases actual bottom-hole pressure is much lower when injection takes place in depleted oil or gas reservoirs (IAE 2003). However, in the case of potential future commercial CO<sub>2</sub> injections from an emitting power plant, the injection will take place at a much larger scale, and therefore other issues, such as potential for fault reactivation and the long-term sealing performance, may be limiting factors for the admissible overpressure (Streit and Hillis 2004; Hawkes et al. 2005; Lucier et al. 2006; Li et al. 2006; Rutqvist et al. 2007, 2008).

Lucier et al. (2006) performed one of the first site-specific geomechanics and injectivity studies, related to carbon capture and storage at the American Electric Power's (AEP) 1.3-GW Mountaineer Power Plant in New Haven, West Virginia. Lucier et al. (2006) completed a coupled fluid flow and geomechanical analysis of the Rose Run Sandstone, a potential injection zone located at a depth of about 2,500 m. They found that injectivity would be quite limited as a result of limited thickness and low to moderate permeability. They estimated that for a single injection well, the formation could take only

a small fraction of the Mountaineer emissions (7 Mt/year), even when applying a relatively high injection pressure (limited to a magnitude just below the fracturing gradient). Moreover, the analysis indicated that induced seismicity in the caprock could occur with a slight increase in pressure if optimally oriented faults would be present (Lucier et al. 2006). However, the site is overlain by multiple low-permeability layers of shales and permeable strata. Consequently, even if a minor fault were reactivated in the caprock just above the injection zone, and if such reactivation would open a new flow path, the overlying multiple shale layers could provide sufficient protection from upward migration of the CO<sub>2</sub> (Gupta et al. 2011). Since 2009, some CO<sub>2</sub> injection has commenced within a 20 MW CO<sub>2</sub> capture and storage Product Validation Facility (PVF). The results showed that the Rose Run Sandstone indeed has limited permeability thickness and suffers from a relatively low fracturing gradient. However, another rock unit, the Copper Ridge Dolomite, with thin vuggy dolomite interbed, had about 100 times higher permeability-thickness (Gupta et al. 2011). It was concluded that the vuggy zones in the Copper Ridge Dolomite have significant local storage potential and likely also to offer regional-scale storage. Nevertheless, in July 2011, the Mountaineer project was placed on hold by AEP, because of uncertain economic and policy conditions.

The In Salah CO<sub>2</sub> storage project is also a prime example with regard to injectivity management. As mentioned, the injection takes place at a depth of about 1.8–1.9 km, into a relatively low-permeability, 20 m thick, water-filled Carboniferous, fractured sandstone (Wright 2011; Mathieson et al. 2011). To ensure adequate injectivity and CO<sub>2</sub> flow rates across the low-permeability sand face, it was decided to use long-reach (about 1–1.5 km) horizontal injection wells. Moreover, the horizontal injection wells were oriented parallel to the direction of the minimum principal horizontal stress and perpendicular to the orientation of the dominant fracture set, which is vertical and strikes roughly NW-SE (Fig. 2). In addition, the three CO<sub>2</sub> injection wells, KB-501, KB-502 and KB-503, were strategically located in areas of high porosity-thickness, as evaluated from a 3D seismic survey (Riddiford et al. 2004; Foster et al. 2004). Reservoir simulations of the CO<sub>2</sub> injection at In Salah indicate dominant fracture flow at least at injection well

KB-502, where the effective permeability exceeds that of the intact sandstone matrix (Bissell et al. 2011).

At In Salah, the maximum wellhead pressure for CO<sub>2</sub> injection was initially set to 18 MPa, in order for the flowing bottom-hole pressure to be below the fracturing pressure of the caprock above the injection zone. This was based on the best estimate of the minimum principal stress depth gradient, which was evaluated from leak-off tests to correspond to a mud weight of 1.7 g/cc (Darling 2006). At 1,800 m depth, this will correspond to about 30 MPa. Using wellbore simulations tools, Bissell et al. (2011) and Rutqvist et al. (2011b) showed that downhole pressure might at times have been higher than 30 MPa, which according Bissell et al. (2011) would exceed the fracturing pressure within the reservoir (but not in the caprock above the injection zone). However, this fracturing pressure refers to the internal wellbore pressure that could fracture the wall of a vertical well considering the rock tensile strength. The most important parameter for maximum sustainable injection pressure is the minimum compressive in situ stress, which for the depth of the injection zone and the caprock above the injection zone can be estimated to about 28.5–30 MPa (Darling 2006; Rutqvist et al. 2011a).

Injection data at one of the injection wells at In Salah (KB-502) have shown a pressure-dependent injectivity (Bissell et al. 2011). In fact, reservoir simulations have shown that it is not possible to match the injection data without considering some type of increasing injectivity with pressure. Bissell et al. (2011) indicated that the injection data showed an abrupt injectivity increase at a bottomhole pressure of 28.6 MPa, which would indicate a sudden fracture opening, with complete loss of contacts between fracture surfaces. The observed permeability changes at KB-502 might also be related to an apparent opening of a deep fractured zone as observed by InSAR ground surface deformation monitoring. The potential for opening of a deep-seated fractured zone will be discussed in more detail in Sect. 9. However, in terms of injectivity management, the maximum well head pressure has now been lowered at KB-502, below the limit of the apparent fracture opening. This is an example of monitoring coupled fluid flow and geomechanical processes leading to important observations regarding the subsurface reservoir performance, and preventative actions.

## 7 Wellbore Integrity

The well design of a deep CO<sub>2</sub> injection well will typically involve at least two strings of casing, including surface casing cemented to the land surface to isolate the well from the shallower aquifers of drinking water (Tsang et al. 2008). The second casing will extend all the way to the injection zone and is cemented to ensure that there is no cross flow between adjacent brine formations. Furthermore, injection tubing is set into a packer, which is a mechanical device set in the well to isolate the injection zone, to ensure that injection via the tubing is emplaced in the target injection zone (Tsang et al. 2008).

Materials, in particular the cement used in the construction of the injection well, must be resistant to corrosion caused by injected CO<sub>2</sub> or formation brines. Because of the corrosive properties of CO<sub>2</sub> and the expected long life of CO<sub>2</sub> injection wells—with an operational period of 25–100 years and a safety period of 1,000 years or more—evaluation of materials for well integrity will be even more stringent. Research has shown that the reaction with typical wellbore cement is too slow to cause leakage in a properly constructed well that is in good condition (Liteanu et al. 2009; Orlic 2009). However, the cement in old abandoned wells could still be a problem, because they may have been completed and abandoned under different standards and practices (Orlic 2009). In fact, abandoned wells from over a century of oil and gas exploration and production have been identified as critical potential leakage paths and generally considered to be one of the greatest risks for upward migration of CO<sub>2</sub> for GCS at a large scale (Nordbotten et al. 2009). For example, recently concerns regarding old wells were a show stopper for a GCS project in the depleted De Lier gas field in The Netherlands (Hofstee et al. 2008). Figure 7 shows the possible leakage paths in an abandoned well, which include preferential flow pathways along rock-cement and casing-cement interfaces, as well as through degraded materials or materials improperly formed during the plugging processes (Gasda et al. 2004; Bachu and Bennion 2009).

Geomechanical processes can impact well integrity both during drilling and completion, as well as during the actual CO<sub>2</sub> injection. Drilling and completion of wells through layers of shale and mudstone requires special attention, because rock failure and deformation

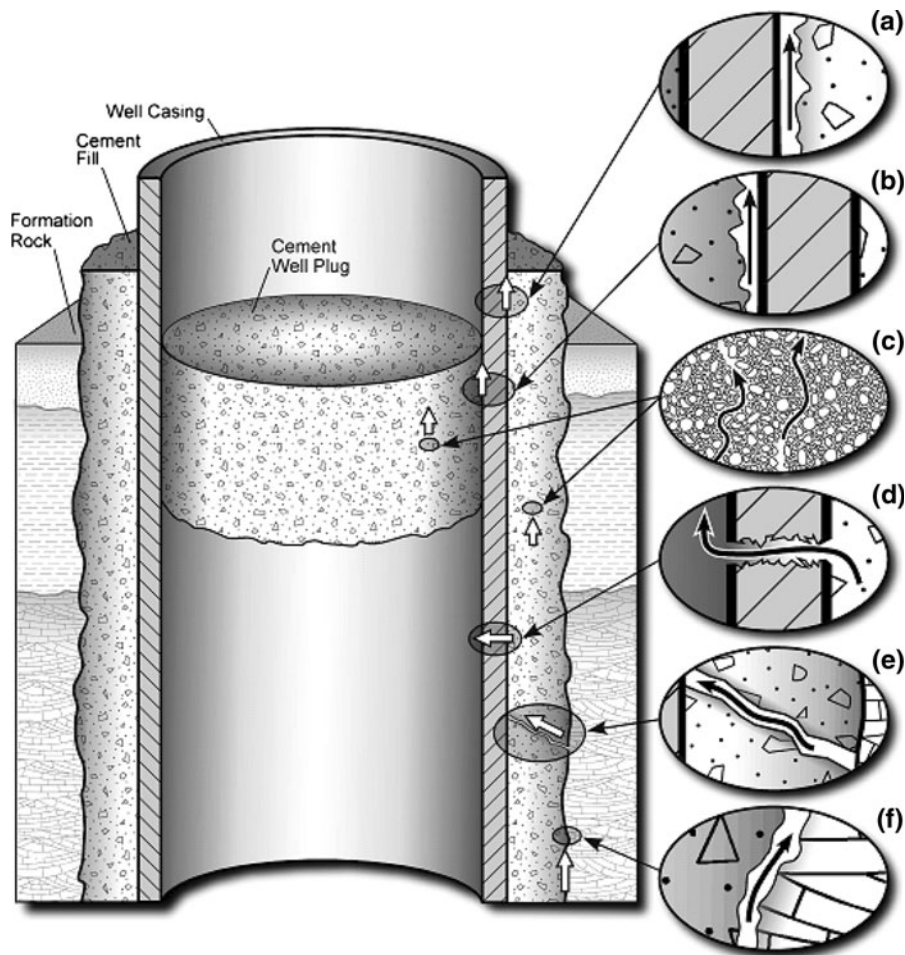


**Fig. 7** Diagrammatic representation of possible leakage pathways through an abandoned well: **a** between casing and cement; **b** between cement plug and casing; **c** through the cement pore

space; **d** through casing; **e** through fractures in cement; and **f** between cement and rock (Gasda et al. 2004)

associated with wellbore instability may damage wellbores, leading to increased permeability and potential leakage paths (Orlic 2009). Pore-fluid chemistry affects chemically sensitive rocks, particularly shales, so that their mechanical properties may change substantially (Dusseault 2011). Radial deformation of the cement sheath is commonly caused by shrinkage during cement hydration, which might result in cracking of the cement sheath or debonding at the rock/cement or cement/casing interface, allowing for radial and vertical migration of fluids (Orlic 2009). During CO<sub>2</sub> injection, changes in reservoir stress and deformations acting on the well assembly will impact the hydraulic aperture of rock-cement and casing-cement interfaces, the most likely pathways for potential CO<sub>2</sub> leakage around abandoned wells (Bachu

and Bennion 2009; Tau et al. 2011). Fractures, if formed in the concrete, will have a rock-fracture-like stress-dependent aperture that could be significantly impacted by coupled chemical degradation once exposed to CO<sub>2</sub> (Huerta et al. 2009; Wigand et al. 2009). Analysis of well geomechanics may require a detailed model including all the mechanical components of the well assembly, linked to reservoir-scale modeling of reservoir pressure, temperature, and stress evolution (Rutqvist et al. 2011b). However, such detailed geomechanical modeling would not be conducted for all the wells at a site. From a geomechanics perspective, the first analysis would be to look at the potential compaction strains and shear strains in the geological layers—and their interfaces—and then evaluate their potential impact on the well assembly.

Analysis of potential CO<sub>2</sub> leakage along wells may then be conducted using separate multiphase flow analysis such as exemplified in the work by Nordbotten et al. (2009), including large number abandoned wells. The analysis of Nordbotten et al. (2009), shows the benefits of multiple caprock layers to mitigate upward leakage rates.

At In Salah, the injection is conducted from state-of-the-art CO<sub>2</sub> injection wells, cased and cemented down to the injection zone. As in any major drilling campaign, a wellbore stability study was performed before the start of drilling. However, severe instability problems were encountered in the first well (KB-501), requiring a major redesign of the program (Foster et al. 2004). Despite this, the well successfully reached a horizontal length of 1,300 m (Foster et al. 2004). The horizontal well sections are 6 inch open hole completions with a pre-slotted liner, oriented optimally with respect to the in situ stress field to avoid borehole instability. CO<sub>2</sub> leakage is unlikely along these state-of-the-art injectors. However, there has been one instance of very small CO<sub>2</sub> leakage along an old appraisal well that was drilled in the 1980s and not cemented across the interval of the CO<sub>2</sub> injection zone (Mathieson et al. 2011; Ringrose et al. 2009; Oldenburg et al. 2009). This highlights the risk with abandoned wells, although in this case the leakage was related to a faulty wellhead and not to geomechanical or geochemical changes caused by CO<sub>2</sub> injection. Nevertheless, the well has since been fully decommissioned, and surface flux and soil gas monitoring will continue around the well for the foreseeable future (Mathieson et al. 2011).

## 8 Caprock Sealing Performance

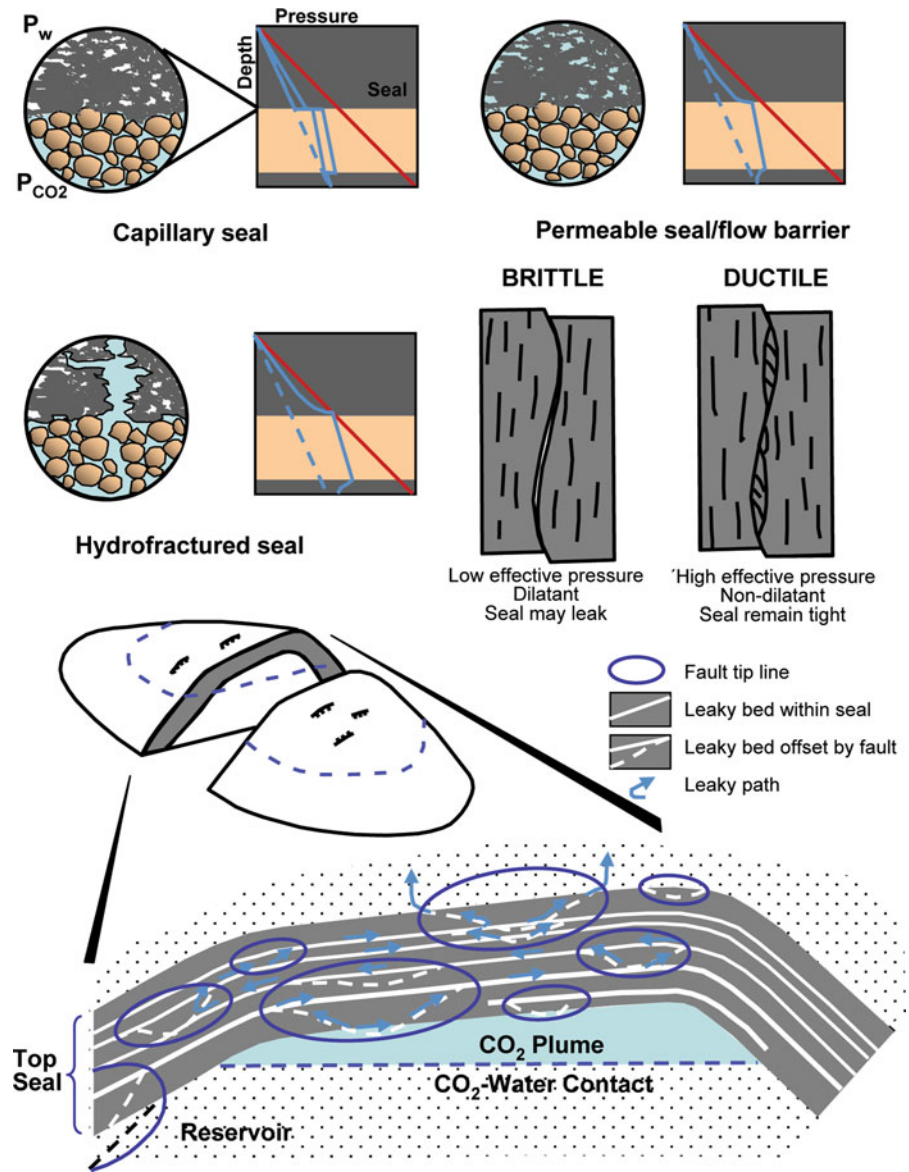
In oil and gas reservoirs, the ability to contain buoyant gas has been proven, but in the case of saline aquifer storage, the sealing properties of the overlying barrier layers may not be well known, or cannot be that well constrained (Orlic 2009). However, experience from both industrial and natural analogues indicates that aquifer storage is indeed a viable option in the right type of settings, contingent upon having an adequate caprock as a top seal. For example, underground gas storage in aquifers is an industrial analogue that like GCS also requires gas injection at an overpressure above ambient hydrostatic water pressure (Katz and

Tek 1981). Among the few reported instances of gas leaks from such facilities, the majority have been problems related to the effectiveness of the caprock (Evans 2009). For example, at the Leroy gas storage facility in Wyoming, observations of gas bubbles at the ground surface suggested a pressure-triggered leakage mechanism involving hydraulic seal changes in the reservoir caprock at an overpressure of a few MPa (Araktingi et al. 1984; Nelson et al. 2005).

For CO<sub>2</sub> storage in deep saline aquifers, most suitable caprocks would be composed of mineralogically homogeneous, thick layers of unfaulted clays, claystones, mudstones, evaporates or salt beds (Chadwick et al. 2008). Ideally, the caprock could be plastic (ductile), in a self-sealing mechanical state, having a high capillary entry pressure and low permeability, as well as being homogenous over a large lateral distance. Analogous to hydrocarbon gas entrapment (Ingram et al. 1997), a capillary entry pressure in excess of any pressure increase due to the CO<sub>2</sub> injection process, or to the buoyancy-driven accumulation of CO<sub>2</sub>, would provide a capillary seal against upward migration of the CO<sub>2</sub> (Fig. 8, upper right). The capillary entry pressure for CO<sub>2</sub>/brine has been evaluated in laboratory tests on rock samples of various types of caprock (Hildenbrand et al. 2004; Chadwick et al. 2008; Carles et al. 2010). Data indicates capillary entry pressure for CO<sub>2</sub> is generally less than that of methane and can range from less than 0.1 up to 10 MPa. Consequently, a CO<sub>2</sub> injection over-pressure of a few MPa might be sufficient to break the capillary barrier. Moreover, caprocks may include discontinuities, such as fractures and faults that may be slightly more permeable, resulting in even lower capillary entry pressure.

If the CO<sub>2</sub> overpressure exceeds the capillary entry pressure, the caprock will act as a permeability barrier in the sense of allowing for Darcy type flow, as shown in Fig. 8, upper right (Ingram et al. 1997). The capillary retention properties are still important, because relative permeability effects could reduce the CO<sub>2</sub> mobility substantially and thereby further reduce the upward buoyancy migration of the supercritical CO<sub>2</sub>. A high injection pressure may cause fracturing or opening of fractures and minor faults that might exist in the caprock, causing a fractured seal as shown in Fig. 8, lower left. Such fracturing can increase the connectivity of permeable interbeds, and if it could propagate across all the overlying sealing

**Fig. 8** Key seal pertaining to top seal integrity for hydrocarbon accumulations according to Ingram et al. (1997) and here applied to GSC in deep sedimentary formations. Capillary seal: the sealing takes place at the CO<sub>2</sub>-water interface and a sharp pressure discontinuity is preserved across the seal. Permeable seal: CO<sub>2</sub> has invaded the seal and a gradient of pressure is maintained throughout. Hydrofractured seal: the CO<sub>2</sub> pressure may become high enough to exceed the fracture strength, and leakage will take place through fractures. *Bottom:* fault-linked leak path. Small faults may link up leaky strata in a top seal, thus forming tortuous, but effective leakage pathways over geologic time



layers, a breach of the top seal may occur (Ingram et al. 1997).

The importance of existing faults and fractures on caprock sealing performance have also been observed related to geological containment of gases in naturally overpressured sediments and gas reservoirs (Poston and Berg 1997; Sibson 2003). In such formations, re-shear of existing cohesionless faults and fractures favorably oriented for frictional reactivation provides the lower bound to overpressures, whereas drainage of conduits by hydraulic-extension fracturing is important only in the case of intact caprock under low differential stress (Sibson 2003). The mechanical

properties of the top seal units are also critical in determining how shear reactivation could change the sealing capacity of a caprock unit (Fig. 8). The shear strength of mudrock and shale could be very low, with friction angle as low as 10 degrees (Ingram and Urai 1999; Hajdarwish 2006). However, despite low strength, a caprock unit consisting of soft plastic (ductile) rock can deform in a plastic but self-sealing way, and might therefore be more favorable than a stiff, brittle and dilatant rock (Nygård et al 2006; Ingram and Urai 1999). Laboratory tests have shown that permeability of fractures in shale may not necessarily increase with shear, but could actually

decrease depending on the stress normal to the fractures (Gutierrez et al. 2000).

Minor faults intersecting a shale caprock might have more complex architecture. For example, faults with offsets on the order of a few meters may have a low permeability fault core of a few centimeters and a more permeable damage zone of several tens of centimeters on each side (Constantin et al. 2004). A fracture network in the damage zone might initially be mineral filled and tight and sealing, but with sufficiently high pressure, fluid may propagate through the fracture network, breaking mineral sealing and thereby opening up a new flow path along the fault's damage zone. Again, geomechanical monitoring of surface deformations and microseismicity is crucial for early detection of unwanted and potentially damaging geomechanical changes, such as reactivation of a fault intersecting the caprock. An example of such monitoring is provided by the In Salah project, in which InSAR monitoring provided indications of a fractured zone opening at the lowermost parts of the caprock; as a result, preventative actions regarding the maximum injection pressure were taken (Mathieson et al. 2011; Bissell et al. 2011). The apparent opening of this deep-seated fractured zone, and geomechanical analysis of that event will be discussed in the next section.

The potential impact of chemical-mechanical coupled processes on caprock sealing performance has been investigated by several research groups, and these investigations have indicated that they would have a minor impact on shales or mudstone caprocks. Studies generally show that for a low-permeability caprock, over thousand of years of exposure, only the lowest few meters of the caprock may be affected by the CO<sub>2</sub>-rich fluid, and the effect on hydraulic and mechanical properties appears to be very small (Gaus et al. 2005; Ojala 2011; Fleury et al. 2010; Hangx et al. 2010; Bildstein et al. 2010). The potential for CO<sub>2</sub> replacing interlayer water leading to shrinkage of the clay minerals is an open issue (Gaus 2010). If such CO<sub>2</sub>-induced shrinkage would occur in the lower parts of a caprock, the horizontal stress might be significantly reduced, and shrinkage cracks could occur. These processes have been mentioned associated with upwelling of CO<sub>2</sub> across thin shale layers at Sleipner (Chadwick et al. 2004). Similar shrinkage effects as a result of mineral dissolution in carbonate-rich rock are also possible (Espinoza et al. 2011). However, most of

the important coupled chemical-mechanical effects are expected to occur along faults and fractures that might exist or were created by high CO<sub>2</sub> injection pressure (Johnson et al. 2005; Gherardi et al. 2007; Andreani et al. 2008; Min et al. 2009; Gaus 2010).

## 9 Potential Fault Reactivation and Notable Seismic Events

The potential for injection-induced fault reactivation and seismicity is an important issue from safety, storage security, and public acceptance perspectives. Since the well known Denver Basin earthquakes associated with underground injection in the 1960s, more cases of injection-induced seismicity have been documented (Nicholson and Wesson 1992; Sminchak and Gupta 2003; Nicol et al. 2011). In general, where injection-induced seismicity has been triggered and monitored, the rates and maximum magnitudes of induced events increase with rising reservoir pressures, total fluid volumes, and injection/extraction rates (Nicol et al. 2011). The similarity between water injection and CO<sub>2</sub> injection in terms of injection induced seismicity at the smaller scale has been indicated by Verdon et al. (2010). Note, though, that of the thousands of injection wells in the world, only a few have induced notable seismic events (Nicholson and Wesson 1992). Thus, while some unfelt microseismic events are to be expected at many sites, notable seismic events may only have the potential to occur at some specific sites, related to local structural geology, stress conditions, rock-mass properties (e.g., soft and ductile or hard and brittle, or fractured), and depending on injection parameters.

Injection-induced seismic events result from the release of stored energy triggered by the increase in fluid pressure from the injection. This is not just limited to seismically active areas, but could also occur within the seismically quiet intraplate crust, such as in the midwestern United States (Zoback 2010). The intraplate brittle crust may often be under a compressive stress state of frictional failure equilibrium and have stored strain energy that can be released by fluid injection, but would otherwise remain stored (Zoback and Zoback 1989; Zoback and Harjes 1997). The reason for these areas being seismically quiet is not the stress field, but its being subjected to a low crustal strain rate. A large-scale CO<sub>2</sub> operation would



likely induce strain rates far exceeding the natural background strain rates within and around the area pressurized by the injection. This is not only of concern in the areas occupied by the stored CO<sub>2</sub> around the injection well, but up to several tens of kilometers away, where significant pressure buildup and interference with other injection wells could occur (Birkholzer and Zhou 2009). Over such a vast area, some significant faults may not be avoidable, and the likelihood and potential consequences of reactivation of such faults needs to be evaluated at any injection site (Morris et al. 2011b).

There are many recent examples of site-specific modeling studies related to predicting the potential for fault reactivation and other geomechanical processes during CO<sub>2</sub> injection. These include the Mountaineer project, West Virginia (Lucier et al. 2006), the Teapot Dome Pilot Field, Wyoming (Chiaramonte et al. 2008, 2011b), the Dogger Carbonates of the Paris Basin (Vidal-Gilbert et al. 2009), a petroleum onshore field, Brazil (Mendes et al. 2010), the In Salah CO<sub>2</sub> storage project, Algeria (Rutqvist et al. 2010; Bissell et al. 2011; Morris et al. 2011a, b; Baroni et al. 2011; Fokker et al. 2011), the Po River plain, Northern Italy (Ferronato et al. 2010), an offshore gas field in the Dutch sector of the North Sea (Orlic et al. 2011), Snøhvit, Barents Sea (Chiaramonte et al. 2011a); Otway, Australia (Vidal-Gilbert et al. 2010), and Ketzin, Germany (Ouellet et al. 2011). The majority of these analyses show that CO<sub>2</sub> injection may induce fault reactivation depending on the applied injection pressure, but there are great uncertainties in the in situ stress field as well as in the assumed strength of fault properties. There might be an estimate of the depth-dependent stress field based on the word stress map, site-specific leak-off tests, and borehole break-out data (Zoback 2007). However, across faults, the local stress field might be significantly different than the average crustal stress field. Also, the fault architecture and shear strength along a fault could be strongly heterogeneous. Therefore, it is very difficult to predict when and exactly at what injection pressure a fault might reactivate. On the other hand, coupled fluid flow and geomechanical modeling may reasonably indicate how the stress field changes as a result of injection, and in which areas the potential for fault reactivation will increase or decrease with the injection. Thus, it can be used to identify areas and individual known faults with the highest potential for reactivation, and thereby

guide the field monitoring. Once field data are available from the actual injection, such data can then be used to recalibrate the coupled models, and then forward modeling can be used for testing new injection parameters.

Calculating and estimating the potential seismic magnitude would be even more difficult. However, it can still be useful to use seismological theories and observations to study what it would take to induce a seismic event of a certain magnitude. For example, Cappa and Rutqvist (2011b) used coupled fluid flow and geomechanical modeling linked with a slip weakening fault model (Kanamori and Brodsky 2001) to calculate fault reactivation and estimation of seismic magnitudes. In seismological theories, quantification of the overall size of an earthquake is generally based on the seismic moment  $M_0$  defined for a ruptured patch on a fault by:

$$M_0 = \mu A d \quad (5)$$

where  $\mu$  is the shear modulus,  $A$  is the rupture area, and  $d$  is the mean slip. Most data compilations find that seismic moment and ruptured fault area are related as  $M_0 \propto A^{3/2}$ , because, at least for a circular rupture,  $M_0$  varies as  $M_0 \propto \Delta\sigma_s A^{3/2}$  (Aki 1967; Eshelby 1957). Then the magnitude ( $M$ ) of an earthquake is given, in terms of seismic moment, by Kanamori and Anderson (1975) as

$$M = (\log_{10} M_0 / 1.5) - 6.1 \quad (6)$$

where the seismic moment,  $M_0$ , is in Nm. Figure 9 shows the results of a model simulation of an injection-induced  $M_w = 3.4$  seismic event (Cappa and Rutqvist 2011b). An  $M_w = 3.4$  seismic event is the equivalent to the maximum magnitude at the aforementioned Basel geothermal project (Håring et al. 2008). In this simulation example, a fault section of 385 m was instantaneously ruptured once the injection overpressure exceeded 10 MPa. Over the ruptured zone, the calculated maximum shear stress drop was 2 MPa, and the maximum slip was 8 cm. The seismic moment and the corresponding magnitude was estimated from Equations (5) and (6) for the calculated mean slip over the ruptured area and the rock shear modulus. In Fig. 10, the results for simulations at different initial stress fields (ratio between horizontal and vertical stress being  $\sigma_h/\sigma_v = 0.6, 0.7$  and  $0.8$ ) were related to other field data from both natural and injection-induced seismicity.

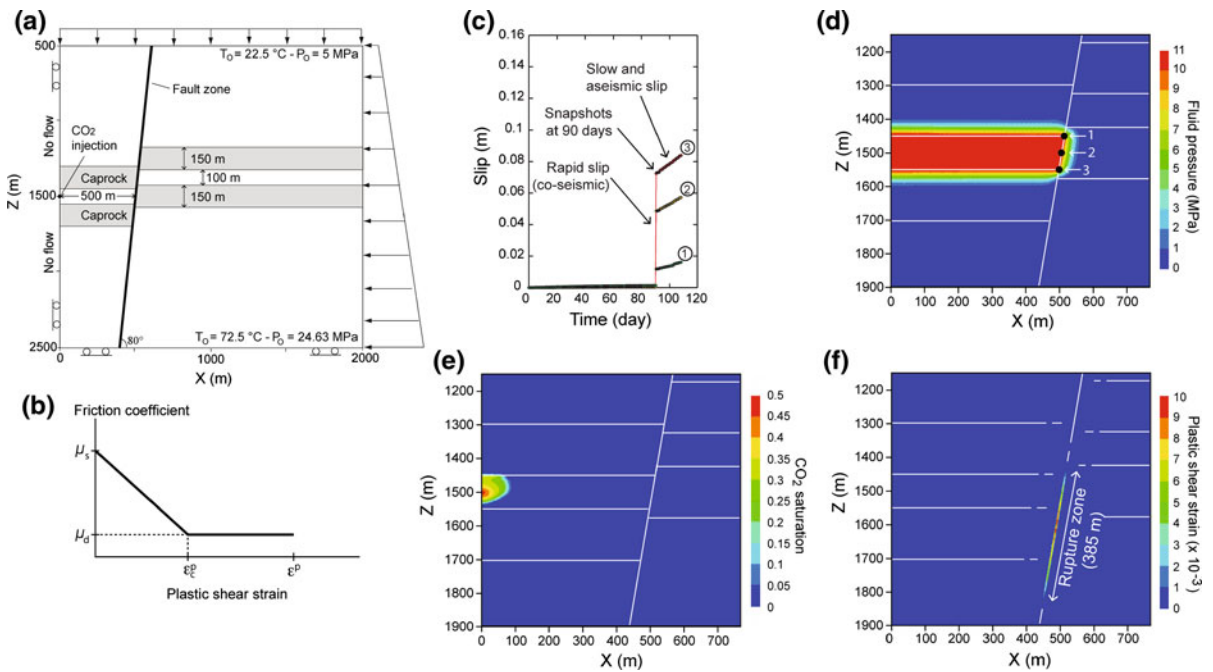


**Fig. 9** Coupled fluid flow and geomechanical simulation of an injection induced fault reactivation corresponding to an  $M_w = 3.4$  seismic event (Cappa and Rutqvist 2011b): **a** numerical model geometry and initial conditions (considered a normal fault with a 125 m offset through a 100 m thick reservoir bounded at the top and the bottom by a 150 m thick caprock); **b** a plastic shear strain-weakening friction law that governs the

propagation of rupture along the fault zone; **c** fault slip versus time at three points located at the (1) top, (2) middle and (3) bottom of the reservoir, respectively (see Fig. 1d for the location). Snapshots of change (relative to the initial state) in **d** fluid pressure, **e**  $CO_2$  saturation, and **f** plastic shear strain at the end of the sudden slip event (after 90 days of  $CO_2$  injection)

**Fig. 10** Seismic scaling relationship after Viegas et al. (2010): source dimension (radius), seismic moment and magnitude. Red and black circles correspond to simulation results of  $CO_2$  injection-induced fault reactivation by Cappa and Rutqvist (2011b)

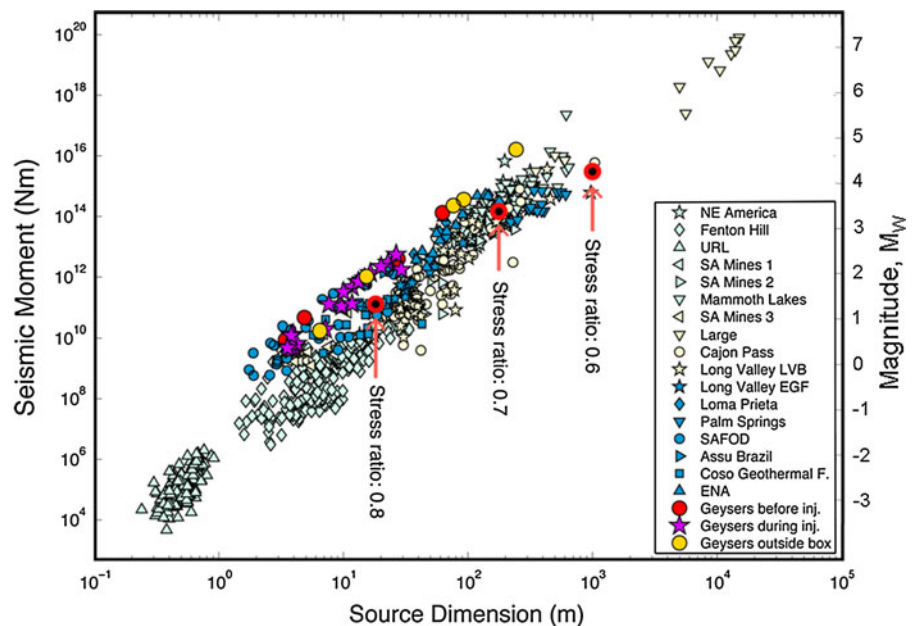


Figure 10 shows that a magnitude 4 event would require a source radius on the order of 1 km. A larger earthquake that could cause significant damage to surface properties, such as a magnitude 6 or 7, would require rupture of a major fault zone with surface rupture on the order of tens of kilometers. However, such major faults are detectable and can thereby be avoided in the site selection, or can be closely monitored during injection.

Another concern is that the reactivation of a minor fault might open up a new flow path for upward migration of CO<sub>2</sub>, as discussed above in Sect. 7. In fact, natural larger-scale releases of CO<sub>2</sub>, such as in volcanic areas, frequently occur along faults, usually along channels or intersections of faults (e.g. Annunziatellis et al. 2008; Cappa et al. 2009). Gas leakage through faults from hydrocarbon reservoirs or underground gas storage facilities has also been inferred from seismic surveys as a “push down” of the seismic signature (Zoback and Zinke 2002; Juhlin et al. 2007). For example, Zoback and Zinke (2002) correlated hydrocarbon leakage through faults observed from seismic signatures to areas where gas production would tend to cause the stress field to move towards failure. Moreover, natural gas seeps are also structurally controlled along faults, such as evident from offshore fluid seepage in the Santa Barbara Basin, California (Eichhubl et al. 2000). These are examples where gas seepage out of a reservoir has been observed, whereas there are thousands of gas fields proven to contain gas for millions of years, with no sudden gas release, even for a large number of gas-producing field areas near

active faults, such as at Ventura Basin, California. Thus, it is very difficult to predict how much fault permeability will change in the case of an injection-induced fault reaction. However, fault permeability could be subject of sensitivity studies and potential permeability changes could perhaps be bounded using fault permeability models (e.g., Cappa and Rutqvist 2011a; Seyedi et al. 2011) and to investigate potential consequence, should a fault be reactivated.

Once again, the In Salah CO<sub>2</sub> storage project provides a prime example for studies of potential fault reactivation during CO<sub>2</sub> injection. As mentioned, the injection pressure is quite substantial (up to 10 MPa, corresponding to about 160% of initial hydrostatic pressure) and the injection zone (the 20 m thick sandstone layer) is intersected by many subvertical minor faults observed from 3D seismic surveys (Iding and Ringrose 2010; Ringrose et al. 2009, 2011). Moreover, InSAR data on ground surface deformation have such a good spatial and temporal resolution that it is possible to detect potential injection-induced fault responses (Mathieson et al. 2011; Morris et al. 2011a, b; Vasco et al. 2010; Bissell et al. 2011). In particular, at injection well KB-502, a more complex surface deformation pattern has been observed, including two parallel uplift lobes rather than one single uplift lobe (Fig. 11). This double-lobe uplift pattern was first interpreted by Vasco et al. (2010) to signify the opening of a linear feature within and around the injection zone, i.e., at around 1,900 m depth.

Vasco et al. (2010) reproduced the double-lobe uplift by modeling an opening of a vertical tensile

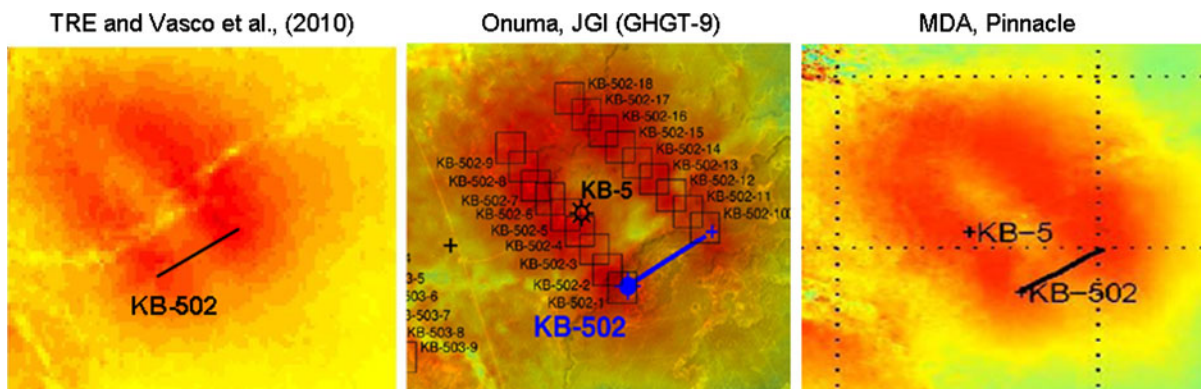
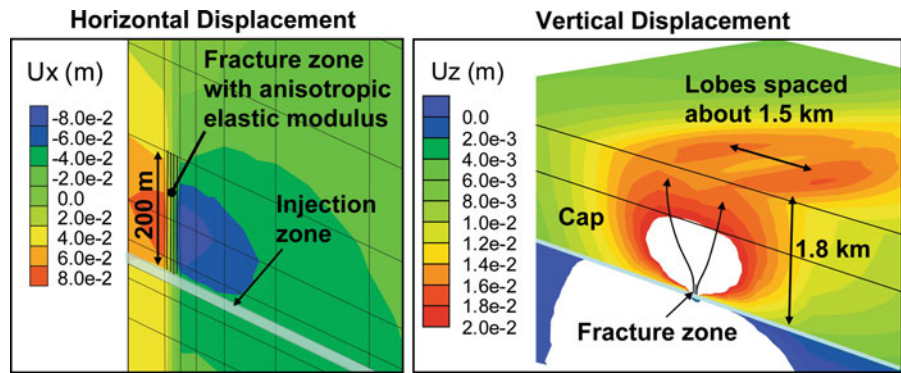


**Fig. 11** Double-lobe uplift response evaluated from InSAR by three independent groups: TRE and Vasco et al. (2010) using PSInSAR (left), and Onuma and Ohkawa (2009) using DInSAR (middle), and MDA (MacDonald, Dettwiler and Associates

Ltd.) Canada and Pinnacle Technology (right). The red contour indicates the largest uplift, which is on the order of 2 cm after about 2 years of injection in KB-502 (Rutqvist et al. 2011b)

**Fig. 12** Forward coupled numerical modeling of CO<sub>2</sub> injection, with pressure inflation of the vertical fracture zone, which results in a double-lobe uplift response on the ground surface similar to observations shown in Fig. 10 (Rutqvist et al. 2011b)



feature at the depth of the injection zone. Similarly, using multiphase fluid-flow and geomechanical numerical modeling, Rutqvist et al. (2011a) as well as Morris et al. (2011a) also concluded that the opening of a vertical feature could explain the observed double-lobe uplift. For example, in Rutqvist et al. (2011a), the vertical feature was modeled as a zone of fractured rock about 50 m wide having a strongly anisotropic elastic modulus (Fig. 12a). According to this model, fluid pressure gradually inflates the vertical fracture zone, which expands laterally to a maximum displacement (x-displacement shown in Fig. 12a) of about 8 cm on each side of the fractured zone. Using such an approach, a double-lobe response similar to the one observed in the field could be reproduced, with a maximum uplift magnitude of

about 2 cm after 2 years of injection, and the two uplift lobes laterally spaced about 1.5 km (Fig. 12b).

More recently, a 3D seismic survey indicated that such a fractured zone may indeed intersect injection well KB-502, and a linear feature is visible in the seismic signature up to a few hundred meters above the injection zone (Gibson-Poole and Raikes 2010; Wright 2011). In fact, the location and orientation of the linear feature seen on the 3D seismic image agrees very well with predictions from the inverse semi-analytic deformation analysis done by Vasco et al. (2010) long before the 3D seismic results were available. The opening is aligned precisely parallel with the dominant fracturing orientation, exactly perpendicular to the minimum compressive principal stress, and is well correlated with the double-lobe

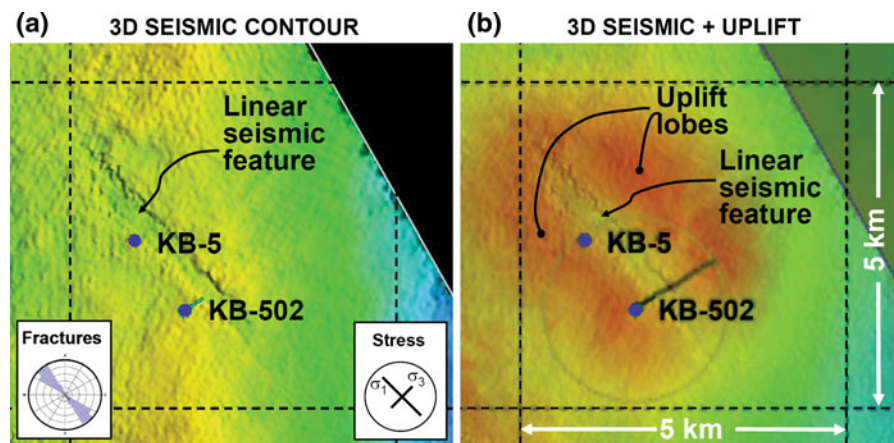


**Fig. 13** Results from 2009 3D seismic survey in northern Kechba, showing a deep linear feature and its correlation with surface uplift, natural fractures, and stress orientation: **a** 3D seismic contour extracted from Gibson-Poole and Raikes (2010) and Wright (2011) showing contour layer at the top of the C20.1 unit, about 150 m above injection zone (at a depth of about 1.7 km), and **b** 3D seismic contour results overlain by ground

surface uplift evaluated from InSAR data of MDA and Pinnacle Technology (Wright 2011). In **a** red and yellow correspond to high elevation, whereas blue corresponds to low elevation, indicating a push down in the seismic signature along the linear feature. In **b**, red contour represents the maximum uplift, on the order of 2 cm, consistent with Fig. 11

uplift on the ground surface (Fig. 13). This very precise linear alignment may indicate the opening of fractures (which exist in the lower part of the caprock) rather than opening or reactivation of a fault. Moreover, the linear feature seen on the image is several hundred meters wide, hence not indicating opening of a single fracture, but rather it might be opening of a fractured zone that is pressure inflated and saturated with CO<sub>2</sub>. Unfortunately, a seismic monitoring network was not in place at the time of the first double-lobe ground-surface response, which occurred gradually over many months. Currently, a number of research groups are working on refining the geomechanical modeling and analysis of this linear feature, and to possibly determine how far up from the injection zone it might have propagated. It is the current understanding that it has not propagated above the defined boundaries of the storage complex, hence indicating that no CO<sub>2</sub> has migrated out of the storage complex (Oldenburg et al. 2009). Moreover, to date, no anomalies have been noted from the soil gas, surface flux, shallow aquifer, or microbiology monitoring work (Mathieson et al. 2011).

Finally, note that the injection zone at In Salah is intersected by a number of faults that theoretically could be close to being reactivated in strike-slip shear (Morris et al. 2011a). These minor faults may extend into immediate caprock horizon, but there are no faults mapped extending from the injection zone through the caprock and into the shallow potable water aquifer. The faults appear to have some effect on the fluid flow and the ground surface uplift pattern (Ringrose et al. 2011, Morris et al. 2011a). However, to date, the CO<sub>2</sub> injection operation at In Salah has not resulted in any felt seismic event and InSAR surface deformations do not indicate substantial strike-slip shear movements. For example, if a fault did reactivate in a strike-slip shear movement of a few centimeters or more, it should be visible on the InSAR surface deformation data. The fact that faults have not been substantially reactivated in strike-slip could indicate that the reservoir pressure is not sufficiently high to cause such strike-slip fault reactivation. However, even if the reservoir pressure were sufficiently high, the faults may be prevented to slip as a result of mechanical resistance from the surrounding rock. Note that only a small (20 m thick) part of the faults intersecting the injection zone might be pressurized, whereas parts of the fault planes above and below the injection zone

might not be pressurized. The faults could thereby be mechanically restricted from substantial strike-slip movements. Nevertheless, the In Salah is another example of an injection operation in which no felt seismic events occur, and for the development of GCS at a larger scale, there is a need to further develop methods for identifying and distinguishing such sites from those that would be more prone to injection-induced seismicity.

## 10 Concluding Remarks and Recommendations

The importance of the geomechanical processes and modeling associated with geologic CO<sub>2</sub> storage can hardly be overemphasized. In particular, recent concerns about the potential for injection-induced fault reactivation and notable (felt) seismic events are key geomechanical issues that need to be addressed before commercial scale GCS operations can be deployed at a large scale. Although no felt seismic event has been reported from any of the current CO<sub>2</sub> storage projects, it should be recognized that potential future commercial GCS operations from large power plants will require injection at a much larger scale. Geomechanical modeling can certainly be used to guide the site selection and evaluate the potential for injection-induced fault reactivation and seismic events, but as mentioned, it is difficult to predict such an event and its magnitude. The main uncertainties are the in situ stress field and large-scale geomechanical properties and their distributions. It is the large-scale pressure buildup, associated crustal straining, and potential undetected faults that might be of greatest concern. The risk is generally expected to increase with injection volume, since this will increase the possibility that the expanding reservoir pressure reaches critically stressed faults of larger dimensions. To deal with this issue, a best-practice framework is needed for the site investigations. This could involve documentation of the historical natural seismicity, assessment of the potential for induced seismicity, and recommended steps for mitigation of the risk of the induced seismicity, as well as addressing the human element (Myer and Daley 2011).

Notwithstanding the potential for triggering notable (felt) seismic events, the potential for buoyancy-driven CO<sub>2</sub> to reach potable ground water and the ground surface is an important issue from safety and

storage-efficiency perspectives. Much depends on the caprock and overburden fluid flow properties and also how these might change as a result of geomechanical changes. For large-scale CO<sub>2</sub> storage in deep saline aquifers, it appears that substantial overpressure may be required—lower than the fracturing pressure of the caprock, but perhaps exceeding the caprock's capillary entry pressure and the caprock would then act as a permeability barrier. We know from aforementioned natural and industrial analogues that fractures and faults in the caprock are important, and pressure-induced reshear of such fractures and faults could give rise to increased gas seepage sufficient to reduce the storage pressure over geologic time (Sibson 2003). This might be a small change in permeability and seepage when related to CO<sub>2</sub> storage, taken over a time period of 100 or 1,000 years. Still, such changes and potentially increased CO<sub>2</sub> seepage could reduce the effectiveness of a CO<sub>2</sub> storage operation.

Considering potential issues related to geomechanical changes associated with large-scale CO<sub>2</sub> injection operations, a staged, learn-as-you-go approach, in a multibarrier repository would be recommended. Such an approach would include the following components: (1) selecting a site with an overburden of multiple low-permeability layers, providing a multiple barrier system, (2) carefully designing and regulating the injection pressure based on estimated in situ stress to avoid damaging geomechanical changes (3) conducting longer-term injection tests using water or CO<sub>2</sub> combined with monitoring of geomechanical changes (such as ground surface deformations and microseismicity) to evaluate the potential for induced seismicity and to calibrate geomechanical models, (4) redesigning injection parameters and gradually ramping up the CO<sub>2</sub> injection rate under continuous monitoring of geomechanical changes, (5) conducting long-term operational injection with continuous monitoring of geomechanical changes for early detection of potentially damaging geomechanical changes and for tracking of underground fluid movements.

In this staged, learn-as-you-go approach, the monitoring of geomechanical changes (such as ground-surface deformations and induced microseismicity) is vital for tracking underground fluid pressure evolution, possibly detecting emerging fault reactivations, and providing an early detection of potential migration out of the storage complex. As mentioned above, the use of such monitoring and management of significant

geomechanical changes has been demonstrated at the In Salah CO<sub>2</sub> storage project. A staged approach with an initially longer-term injection, accompanied by seismic and surface-deformation monitoring can be used to determine how prone the site is to triggering notable (felt) seismicity, and can provide the necessary data on site-specific seismicity (if any) to make predictions for long-term operational conditions. For example, at In Salah, it appears that many minor faults within the reservoir could be close to being critically stressed for strike-slip reactivation, but monitoring during injection shows only some microseismic events, while no felt events has occurred. During CO<sub>2</sub> operation, geomechanical monitoring, with early detection of unwanted geomechanical changes, enables preventative actions, e.g., reducing injection pressure. This has also been demonstrated in practice at In Salah. However, at injection operations where significant induced seismicity occurs, it is recommended to make such changes in the injection parameters gradually, avoiding abrupt changes, because many of the largest seismic events at other types of underground injections (such as the aforementioned Basel project) have occurred after shutting down the injection.

Finally, GCS beneath a system of multilayered overburden can be very beneficial from storage security perspective, because it provides multiple flow barriers against upward buoyancy-driven CO<sub>2</sub> migrations, which may be crucial in the event of unexpected reactivation of deep faults that might cross the storage unit. Thus, even if a deep fault is reactivated, and if such reactivation would lead to a local flow path out of the intended storage unit, the overlying low permeability layers could still provide necessary protection by impeding upward migration of the CO<sub>2</sub>.

**Acknowledgments** This work was jointly supported by the Assistant Secretary for Fossil Energy, Office of Natural Gas and Petroleum Technology, through the National Energy Technology Laboratory, and the In Salah JIP and their partners BP, Statoil, and Sonatrach under the U.S. Department of Energy Contract No. DE-AC02-05CH11231. Technical review comments by Allan Mathieson and Rob Bissell of the In Salah JIP, U.K.; Bogdan Orlic at TNO, Utrecht, The Netherlands; Frederic Cappa, at the Berkeley Lab; Pengzhi Pan at the Chinese Academy of Sciences, Wuhan, China; Shinsuke Nakao and Takashiro Funatsu at AIST, Tsukuba, Japan; Ki-Bok Min and Jaewon Lee at the Seoul National University, Korea; as well as editorial review by Dan Hawkes at the Berkeley Lab are all greatly appreciated.

**Open Access** This article is distributed under the terms of the Creative Commons Attribution Noncommercial License which permits any noncommercial use, distribution, and reproduction in any medium, provided the original author(s) and source are credited.

## References

- Abbot A (2004) Plans resurrected to raise Venice above the encroachment sea. *Nature* 427:184
- Aki K (1967) Scaling law of seismic spectrum. *J Geophys Res* 72:1217–1231
- Andreani M, Gouze P, Luquot L, Jouanna P (2008) Changes in seal capacity of fractured claystone caprocks induced by dissolved and gaseous CO<sub>2</sub> seepage. *Geophys Res Lett* 35:L14404
- Annunziatellis A, Beaubien SE, Bigi S, Ciotoli G, Coltella M, Lombardi S (2008) Gas migration along fault systems and through the vadose zone in the Latera caldera (central Italy): implications for CO<sub>2</sub> geological storage. *Int J Greenh Gas Control* 2:353–372
- Araktingi RE, Benefield ME, Bessenyei Z, Coats KH, Tek MR (1984) Leroy storage facility, Uinta County, Wyoming—a case history of attempted gas migration control. *J Petrol Technol* 36(1):132–140
- Bachu S (2008) CO<sub>2</sub> storage in geological media: role, means, status and barriers to deployment. *Prog Ener Combust Sci* 34:254–273
- Bachu S, Bennion DB (2009) Experimental assessment of brine and/or CO<sub>2</sub> leakage through well cements at reservoir conditions. *Int J Greenh Gas Control* 3:494–501
- Baisch S, Vörös R, Rotherth E, Stang H, Jung R, Schellschmidt R (2010) A numerical model for fluid injection induced seismicity at Soultz-sous-Forêts. *Int J Rock Mech Min Sci* 47:405–413
- Baroni A, Estublier E, Deflandre JP, Daniel JM (2011) Modeling surface displacements associated with CO<sub>2</sub> re-injection at Krechba. In: Proceedings of 45th US Rock mechanics/geomechanics symposium, San Francisco, CA, June 26–29
- Benson SM, Cole DR (2008) CO<sub>2</sub> sequestration in deep sedimentary formations. *Elements* 4:325–331
- Bickle MJ (2009) Geological carbon storage. *Nature Geosci* 2(December 2009):815–819
- Bildstein O, Kervévan C, Lagneau V, Delaplace P, Crédoz A, Audigane P, Perfetti E, Jacquemet N, Jullien M (2010) Integrative modeling of caprock integrity in the context of CO<sub>2</sub> storage: evolution of transport and geochemical properties and impact on performance and safety assessment. *Oil Gas Sci Technol Rev IFP* 65:485–502
- Birkholzer JT, Zhou Q (2009) Basin-scale hydrogeologic impacts of CO<sub>2</sub> storage: capacity and regulatory implications. *Int J Greenh Gas Control* 3:745–756
- Bissell RC, Vasco DW, Atbi M, Hamdani M, Okwelegbe M, Goldwater MH (2011) A full field simulation of the In Salah gas production and CO<sub>2</sub> storage project using a coupled geo-mechanical and thermal fluid Flow simulator. *Energy Procedia* 4:3290–3297
- Bower KM, Zyvoloski G (1997) A numerical model for thermo-hydro-mechanical coupling in fractured rock. *Int J Rock Mech Min Sci* 34:1201–1211
- Burch DN, Daniels J, Gillard M, Underhill W, Exler VA, Favoretti L, Le Calves J, Lecerf B, Potapenko D, Maschio L, Morales JA, Samuelson M, Weimann MI (2009) Live hydraulic fracturing monitoring and diversion. *Oilfield Rev* 21:18–31
- Cappa F, Rutqvist J (2011a) Modeling of coupled deformation and permeability evolution during fault reactivation induced by deep underground injection of CO<sub>2</sub>. *Int J Greenh Gas Control* 5:336–346
- Cappa F, Rutqvist J (2011b) Impact of CO<sub>2</sub> geological sequestration on the nucleation of earthquakes. *Geophys Res Lett* 38:L17313
- Cappa F, Rutqvist J, Yamamoto K (2009) Modeling crustal deformation and rupture processes related to upwelling of deep CO<sub>2</sub> rich fluids during the 1965–1967 Matsuhiro earthquake swarm in Japan. *J Geophys Res* 114:B10304
- Carles P, Bachaud P, Lasseur E, Berne P, Bretonnier P (2010) Confining properties of carbonated Dogger caprocks (Parisian Basin) for CO<sub>2</sub> storage purpose. *Oil Gas Sci Technol Rev IFP* 65:461–472
- Castelletto N, Ferronato M, Gambolati G, Putti M, Teatini P (2008) Can Venice be raised by pumping water underground? A pilot project to help decide. *Water Resour Res* 44:W01408
- Chadwick RA, Arts R, Eiken O, Kirby GA, Lindeberg E, Zweigel P (2004) 4D seismic imaging of an injected CO<sub>2</sub> plume at the Sleipner Field, central North Sea. *Geol Soc Lon Mem* 29:311–320
- Chadwick A, Arts R, Bernstone C, May F, Thibeau S, Zweigel P (2008) Best practice for the storage of CO<sub>2</sub> in saline aquifers: observations and guidelines from the SACS and CO<sub>2</sub>STORE projects. British Geological Survey, Keyworth
- Chalaturnyk RJ (2007) Geomechanical characterization of the Weyburn field for geological storage of CO<sub>2</sub>. In: Proceedings of 1st Canada-US rock mechanics symposium, Vancouver, Canada, 27–31 May 2007
- Chiaromonte L, Zoback MD, Friedmann J, Stamp V (2008) Seal integrity and feasibility of CO<sub>2</sub> sequestration in the Teapot Dome EOR pilot: geomechanical site characterization. *Environ Geol* 54:1667–1675
- Chiaromonte L, White JA, Johnson S (2011a) Preliminary geomechanical analysis of CO<sub>2</sub> injection at Snøhvit, Norway. In: Proceedings of 45th US Rock mechanics/geomechanics symposium, San Francisco, CA, June 26–29
- Chiaromonte L, Zoback M, Friedmann J, Stamp V, Zahm C (2011b) Fracture characterization and fluid flow simulation with geomechanical constraints for a CO<sub>2</sub>-EOR and sequestration project Teapot Dome oil field, Wyoming, USA. *Energy Procedia* 4:3973–3980
- CMG (2003) User's guide STARS. Computer Modelling Group Ltd., Calgary
- Comerlati A, Ferronato M, Gambolati G, Putti M, Teatini P (2006) Fluid-dynamic and geomechanical effects of CO<sub>2</sub> sequestration below the Venice Lagoon. *Environ Eng Geosci* 12:211–226
- Constantin J, Peyaud JB, Vergély P, Pagel M, Cabrera J (2004) Evolution of structural fault permeability in argillaceous

- rocks in a polyphased tectonic context. *Phys Chem Earth* 29:25–41
- Darling T (2006) Krechba overburden review. In: Sala JIP report, April 2006
- Deng H, Dai Z, Jiao Z, Stauffer PH, Surdam RC (2011) Simulation of CO<sub>2</sub> sequestration at Rock Spring uplift, Wyoming: heterogeneity and uncertainties in storage capacity, injectivity and leakage. *Int J Greenh Gas Control* (submitted April 2011)
- Dusseault MB (2011) Geomechanical challenges in petroleum reservoir exploitation. *KSCE J Civ Eng* 15:669–678
- Eichhubl P, Greene HC, Naehr T, Maher TN (2000) Structural control of fluid flow: offshore fluid seepage in the Santa Barbara Basin, California. *J Geoch Explor* 69–70:545–554
- Eiken O, Ringrose P, Hermanrud C, Nazarian B, Torp TA, Hier L (2011) Lessons learned from 14 years of CCS operations: Sleipner, In Salah and Snøhvit. *Energy Procedia* 4:5541–5548
- Eshelby JD (1957) The determination of the elastic field of an ellipsoidal inclusion and related problems. *Proc R Soc London* 241:376–396
- Espinoza DN, Kim SH, Santamarina JC (2011) CO<sub>2</sub> geological storage—geotechnical implications. *KSCE J Civ Eng* 15:707–719
- Evans DJ (2009) A review of underground fuel storage events and putting risk into perspective with other areas of the energy supply chain. *Geol Soc Spec Publ* 313:173–216
- Ferronato M, Gambolati G, Janna C, Teatini P (2010) Geomechanical issues of anthropogenic CO<sub>2</sub> sequestration in exploited gas fields. *Energy Convers Manage* 51:1918–1928
- Fjær E, Holt RM, Horsrud P, Raaen AM, Risnes R (2008) *Petroleum related rock mechanics*, 2nd edn. Elsevier, Amsterdam
- Fleury M, Pironon J, Le Nindre YM, Bildstein O, Berne P, Lagneau V, Broseta D, Pichery T, Fillacier S, Lescanne M, Vidal O (2010) Evaluating sealing efficiency of caprocks for CO<sub>2</sub> storage: an overview of the geocarbone-integrity program and results. *Oil Gas Sci Technol Rev IFP* 65: 435–444
- Fokker PA, Orlic B, Van der Meer LGH, Geel CR (2011) Geomechanical modelling of surface uplift around well KB-502 at the In Salah CO<sub>2</sub> storage site. *SPE—73rd European association of geoscientists and engineers conference and exhibition 2011*, pp 5380–5384
- Foster L, Aidoo A, Tourqui A, Castle-Smith A, Mezdour J, Taylor M (2004) Multi-disciplinary teamwork delivers outstanding Krechba Horizontal well performance. *The 6th Journées Scientifiques et techniques*, 20 to 22 June 2004, Algiers, Algeria
- Gasda SE, Bachu S, Celia MA (2004) The potential for CO<sub>2</sub> leakage from storage sites in geological media: analysis of well distribution in mature sedimentary basins. *Environ Geol* 46(6–7):707–720
- Gaus I (2010) Role and impact of CO<sub>2</sub>—rock interactions during CO<sub>2</sub> storage in sedimentary rocks. *Int J Greenh Gas Control* 4:73–89
- Gaus I, Azaroual M, Czernichowski-Laurio I (2005) Reactive transport modelling of the impact of CO<sub>2</sub> injection on the clayey cap rock at Sleipner (North Sea). *Chem Geol* 217:319–337
- Geertsma J (1973) Land subsidence above compacting oil and gas reservoirs. *J Petrol Tech* 25:734–744
- Gherardi F, Xu T, Pruess K (2007) Numerical modeling of self-limiting and self-enhancing caprock alteration induced by CO<sub>2</sub> storage in a depleted gas reservoir. *Chem Geol* 244:103–129
- Gibson-Poole CM, Raikes S (2010) Enhanced understanding of CO<sub>2</sub> storage at Krechba from 3D seismic. In: *Proceedings of 9th annual conference on carbon capture and sequestration*, Pittsburgh, Pennsylvania, May 10–13, 2010
- Goerke UJ, Park CH, Wang W, Singh AK, Kolditz O (2011) Numerical simulation of multiphase hydromechanical processes induced by CO<sub>2</sub> injection into deep saline aquifers. *Oil Gas Sci Technol Rev IFP* 66:105–118
- Gunter WD, Bachu S, Benson SM (2004) The role of hydrogeological and geochemical trapping in sedimentary basins for secure geological storage for carbon dioxide. In: Baines SJ, Worden RH (eds) *Geological storage of carbon dioxide*. *Geol Soc Spec Publ* 233:129–145
- Gupta N, Gupka NRO, Spitznogle G, Bollinger R, Bhattacharya I (2011) Geologic storage and monitoring at American Electric Power's Mountaineer plant—what have we learned after one year of injection. In: *Proceedings of 10th annual conference on carbon capture and sequestration*, Pittsburgh, Pennsylvania, May 2–5, 2011
- Gutierrez M, Øinob LE, Nygård R (2000) Stress-dependent permeability of a de-mineralised fracture in shale. *Mar Pet Geol* 17:895–907
- Hajdarwish AM (2006) *Geologic controls of shear strength behavior of mudrocks*. PhD Thesis, Kent State University, Department of Geology, Ohio, USA
- Hangx SJT, Spiers CJ, Peach CJ (2010) Mechanical behavior of anhydrite caprock and implications for CO<sub>2</sub> sealing capacity. *J Geophys Res* 115:B07402
- Häring MO, Schanz U, Ladner F, Dyer BC (2008) Characterisation of the Basel 1 enhanced geothermal system. *Geothermics* 37:469–495
- Hawkes CD, McLellan PJ, Bachu S (2005) Geomechanical factors affecting geological storage of CO<sub>2</sub> in depleted oil and gas reservoirs. *J Can Pet Technol* 44:52–61
- Hildenbrand A, Schlomer S, Kroos MK (2004) Gas breakthrough experiments on pelitic rocks: comparative study with N<sub>2</sub>, CO<sub>2</sub> and CH<sub>4</sub>. *Geofluids* 2:61–80
- Hofstee C, Seeberge F, Orlic B, Mulders F, Van Bergen F, Bisschop R (2008) The feasibility of effective and safe carbon dioxide storage in the De Lier gas field. *First Break* 26:53–57
- Huerta NJ, Bryant SL, Strazisar BR, Kutchko BG, Conrad LC (2009) The influence of confining stress and chemical alteration on conductive pathways within wellbore cement. *Energy Procedia* 1:3571–3578
- Iding M, Ringrose P (2010) Evaluating the impact of fractures on the performance of the In Salah CO<sub>2</sub> storage site *Int J Greenhouse Gas. Control* 4:242–248
- IEA (2003) *Acid gas injection: a study of existing operations*. IAE Greenhouse Gas R&D Programme Report No PH4/18, April 2003
- Ingram GM, Urai JL (1999) Top-seal leakage through faults and fractures: the role of mudrock properties. *Geol Soc Spec Publ* 158:125–135



- Ingram GM, Urai JL, Naylor MA (1997) Sealing processes and top seal assessment. In: Moller-Pedersen P, Koestler AG (eds) Hydrocarbon seals: importance for exploration and production. Norwegian Petroleum Society (NPF) Special Publication 7:165–175
- IPCC (Intergovernmental Panel on Climate Change) (2005) In: Metz B, Davidson O, de Coninck HC, Loos M, Mayer LA (eds) Special report on carbon dioxide capture and storage. Cambridge University Press, Cambridge
- Johnson JW, Nitao JJ, Morris JP (2005) Reactive transport modeling of cap rock integrity during natural and engineered CO<sub>2</sub> storage. In: Benson S (ed) CO<sub>2</sub> capture project summary, vol 2. Elsevier, Amsterdam
- Juhlin C, Zinck-Jørgensen RG, Cosma C, Kazemeini H, Juhonjuntti N, Lüth S, Norden B, Förster A (2007) 3D baseline seismics at Ketzin, Germany: the CO<sub>2</sub>SINK project. *Geophysics* 72(5):B121–B132
- Kanamori H, Anderson DL (1975) Theoretical basis of some empirical relations in seismology. *Bull Seism Soc Am* 65: 1073–1095
- Kanamori H, Brodsky EE (2001) The physics of earthquakes. *Physics Today* 54:34–40
- Katz DL, Tek MR (1981) Overview on underground storage of natural gas. *J Pet Technol* 33:943–951
- Kvamme B, Liu S (2009) Reactive transport of CO<sub>2</sub> in saline aquifers with implicit geomechanical analysis. *Energy Procedia* 1:3267–3274
- Le Guen Y, Renard F, Hellmann R, Brosse E, Collombet M, Tisserand D, Gratier J-P (2007) Enhanced deformation of limestone and sandstone in the presence of high Pco<sub>2</sub> fluids. *J Geophys Res* 112:B05421
- Li Q, Wu ZS, Li XC, Ohsumi T, Koide H (2002) Numerical simulation on crust deformation due to CO<sub>2</sub> sequestration in deep aquifers. *J Appl Mech JSCE* 5:591–600
- Li Q, Wu ZS, Bai YL, Yin XC, Li ZC (2006) Thermo-hydro-mechanical modeling of CO<sub>2</sub> sequestration system around fault environment. *Pure Appl Geophys* 163:2585–2593
- Liteanu E, Spiers CJ, Peach CJ (2009) Failure behaviour well-bore cement in the presence of water and supercritical CO<sub>2</sub>. *Energy Procedia* 1:3553–3560
- Lucier A, Zoback M, Gupta N, Ramakrishnan TS (2006) Geomechanical aspects of CO<sub>2</sub> sequestration in a deep saline reservoir in the Ohio River Valley region. *Environ Geosci* 13:85–103
- Mathias SA, Hardisty PE, Trudell MR, Zimmerman RW (2010) Screening and selection of sites for CO<sub>2</sub> sequestration based on pressure buildup. *Int J Greenh Gas Control* 4:108–109
- Mathieson A, Wright I, Roberts D, Ringrose P (2009) Satellite imaging to monitor CO<sub>2</sub> movement at Krechba, Algeria. *Energy Procedia* 1:2201–2209
- Mathieson A, Midgley J, Dodds K, Wright I, Ringrose P, Saoul N (2010) CO<sub>2</sub> sequestration monitoring and verification technologies applied at Krechba, Algeria. *Lead Edge* 29: 216–222
- Mathieson A, Midgley J, Wright I, Saoul N, Ringrose P (2011) In Salah CO<sub>2</sub> Storage JIP: CO<sub>2</sub> sequestration monitoring and verification technologies applied at Krechba, Algeria. *Energy Procedia* 4:3596–3603
- Mendes RA, Costa AM, Sousa Jr LC, Pereira LC (2010) Risks and mitigation problems in a CO<sub>2</sub> injection project for a petroleum onshore field in Brazil. In: Proceedings of 44th US Rock mechanics symposium, Salt Lake City, Utah, USA, June 27–June 30, 2010
- Michael K, Golab A, Shulakova V, Ennis-King J, Allinson G, Sharma S, Aiken T (2010) Geological storage of CO<sub>2</sub> in saline aquifers—a review of the experience from existing storage operations. *Int J Greenh Gas Control* 4:659–667
- Min KB, Rutqvist J, Elsworth D (2009) Chemically and mechanically mediated influences on the transport and mechanical characteristics of rock fractures. *Int J Rock Mech Min Sci* 46:80–89
- Morris JP, Hao Y, Foxall W, McNab W (2011a) In Salah CO<sub>2</sub> Storage JIP: hydromechanical simulations of surface uplift due to CO<sub>2</sub> injection at In Salah. *Energy Procedia* 4: 3269–3275
- Morris JP, Detwiler RL, Friedmann SJ, Vorobiev OY, Hao Y (2011b) The large-scale geomechanical and hydrogeological effects of multiple CO<sub>2</sub> injection sites on formation stability. *Int J Greenh Gas Control* 5:69–74
- Myer LR, Daley TM (2011) Elements of a best practices approach to induced seismicity in geologic storage. *Energy Procedia* 4:3707–3713
- Nelson CR, Evans JM, Sorensen JA, Steadman EN, Harju JA (2005) Factors affecting the potential for CO<sub>2</sub> leakage from geologic sinks. Plains CO<sub>2</sub> reduction (PCOR) partnership. Energy & environment research center, October 2005, University of North Dakota, North Dakota, USA
- Nguyen MT, Bemer E, Dormieux L (2011) Micromechanical modeling of carbonate geomechanical properties evolution during acid gas injection. In: Proceedings of 45th US Rock mechanics/geomechanics symposium, San Francisco, California, USA, June 27–June 30, 2011
- Nicholson C, Wesson RL (1992) Triggered earthquakes and deep well activities. *Pure Appl Geophys* 139:561–578
- Nicol A, Carne R, Gerstenberger M, Christophersen A (2011) Induced seismicity and its implications for CO<sub>2</sub> storage risk. *Energy Procedia* 4:3699–3706
- Nordbotten JM, Kavetski D, Celia M, Bachu S (2009) Model for CO<sub>2</sub> leakage including multiple geological layers and multiple leaky wells. *Environ Sci Technol* 43:743–749
- Nygård R, Gutierrez M, Bratli RK, Høeg K (2006) Brittle–ductile transition, shear failure and leakage in shales and mudrocks. *Mar Pet Geol* 23:201–212
- Odonne F, Ménard I, Massonnat GJ, Rolando JP (1999) Abnormal reverse faulting above a depleting reservoir. *Geology* 27:111–114
- Ohtake M (1974) Seismic activity induced by water injection at Matsushiro, Japan. *J Phys Earth* 22:163–174
- Ojala I (2011) The effect of CO<sub>2</sub> on the mechanical properties of reservoir and cap rock. *Energy Procedia* 4:5392–5397
- Oldenburg CM, Bryant SL, Nicot JP (2009) Certification framework based on effective trapping for geologic carbon sequestration. *Int J Greenh Gas Control* 3:444–457
- Olivella S, Carrera J, Gens A, Alonso EE (1994) Nonisothermal multiphase flow of brine and gas through saline media. *Trans Porous Media* 15:271–293
- Onuma T, Ohkawa S (2009) Detection of surface deformation related with CO<sub>2</sub> injection by DInSAR at In Salah, Algeria. *Energy Procedia* 1:2177–2184
- Orlic B (2009) Some Geomechanical aspects of geological CO<sub>2</sub> sequestration. *KSCE J Civ Eng* 13:225–232

- Orlic B, ter Heege J, Wassing BBT (2011) Assessing the short-term and long-term integrity of top seals in feasibility studies of geological CO<sub>2</sub> storage. Proc 45th US Rock mechanics/geomechanics symposium, San Francisco, California, June 26–29
- Ouellet A, Bérard T, Desroches TJ, Frykman P, Welsh P, Minton PJ, Pamukcu Y, Hurter S, Schmidt-Hattenberger C (2011) Reservoir geomechanics for assessing containment in CO<sub>2</sub> storage: a case study at Ketzin, Germany. Energy Procedia 4:3298–3305
- Plasynski SI, Litynski JT, McIlvried HG, Vikara DM, Srivastava RD (2011) The critical role of monitoring, verification, and accounting for geologic carbon dioxide storage projects. Environ Geosci 18:19–34
- Poston SW, Berg RR (1997) Overpressured gas reservoirs. Society of Petroleum Engineers, Richardson
- Preisig M, Prévost JH (2011) Coupled multi-phase thermoporo-mechanical effects. Case study: CO<sub>2</sub> injection at In Salah, Algeria Int J Greenh Gas Control 5:1055–1064
- Raleigh CB, Healy JH, Bredehoeft JD (1976) An experiment in earthquake control at Rangely, Colorado. Science 191:1230–1237
- Riddiford F, Wright I, Bishop C, Espie T, Tourqui A (2004) Monitoring geological storage: the In Salah gas CO<sub>2</sub> storage project. In: Proceedings of 7th international conference on greenhouse gas control technologies (GHGT-7), Vancouver, Canada, September 5–9, 2004
- Ringrose P, Atbi M, Mason D, Espinassous M, Myhrer Ø, Iding M, Mathieson A, Wright I (2009) Plume development around well KB-502 at the In Salah CO<sub>2</sub> storage site. First Break 27:85–89
- Ringrose P, Roberts DM, Gibson-Poole CM, Clare Bond C, Wightman R, Taylor M, Raikes S, Iding M, Østmo S (2011) Characterisation of the Krechba CO<sub>2</sub> storage site: critical elements controlling injection performance. Energy Procedia 4:4672–4679
- Rohmer J, Olivier B (2010) A response surface methodology to address uncertainties in cap rock failure assessment for CO<sub>2</sub> geological storage in deep aquifers. Int J Greenh Gas Control 4:198–208
- Rohmer J, Seyedi DM (2010) Coupled large scale hydromechanical modelling for caprock failure risk assessment of CO<sub>2</sub> storage in deep saline aquifers. Oil Gas Sci Technol Rev IFP 65:503–517
- Rutledge J, Zhou R, Huang L, McPherson B (2009) Microseismic monitoring of CO<sub>2</sub> injection in the Aneth Oil Field, San Juan County, Utah. The Society of Exploratory Geophysicists (SEG) Summer workshop in Banff, Canada, August 23–27, 2009
- Rutqvist J (2011) Status of the TOUGH-FLAC simulator and recent applications related to coupled fluid flow and crustal deformations. Comput Geosci 37:739–750
- Rutqvist J, Tsang C-F (2002) A study of caprock hydromechanical changes associated with CO<sub>2</sub> injection into a brine aquifer. Environ Geol 42:296–305
- Rutqvist J, Wu Y-S, Tsang C-F, Bodvarsson GA (2002) Modeling approach for analysis of coupled multiphase fluid flow, heat transfer, and deformation in fractured porous rock. Int J Rock Mech Min Sci 39:429–442
- Rutqvist J, Birkholzer J, Cappa F, Tsang C-F (2007) Estimating maximum sustainable injection pressure during geological sequestration of CO<sub>2</sub> using coupled fluid flow and geo-mechanical fault-slip analysis. Energy Convers Manage 48:1798–1807
- Rutqvist J, Birkholzer JT, Tsang C-F (2008) Coupled reservoir-geomechanical analysis of the potential for tensile and shear failure associated with CO<sub>2</sub> injection in multilayered reservoir-caprock systems. Int J Rock Mech Min Sci 45:132–143
- Rutqvist J, Vasco D, Myer L (2010) Coupled reservoir-geomechanical analysis of CO<sub>2</sub> injection and ground deformations at In Salah, Algeria. Int J Greenh Gas Control 4:225–230
- Rutqvist J, Liu H-H, Vasco DW, Pan L, Kappler K, Majer E (2011a) Coupled non-isothermal, multiphase fluid flow, and geomechanical modeling of ground surface deformations and potential for induced micro-seismicity at the In Salah CO<sub>2</sub> storage operation. Energy Procedia 4:3542–3549
- Rutqvist J, Moridis GJ, Grover T, Silpngarmert, Cottett TS, Holdich SA (2011b) Coupled multiphase fluid flow and wellbore stability analysis associated with gas production from oceanic hydrate-bearing sediments (in review)
- Saripalli P, McGrail BP (2002) Semi-analytical approaches to modeling deep well injection of CO<sub>2</sub> for geological sequestration. Energy Convers Manage 43:185–198
- Segall P (1989) Earthquakes triggered by fluid extraction. Geology 17:942–946
- Selvadurai APS (2009) Heave of a surficial rock layer due to pressures generated by injected fluids. Geophys Res Lett 36:L14302
- Seyedi DM, Duceillier A, Vu MN (2011) A two-scale model for simulating the hydromechanical behavior of faults during CO<sub>2</sub> geological storage operation. Proc 45th US Rock mechanics/geomechanics symposium, San Francisco, California, June 26–29, 2011
- Sibson RH (2003) Brittle-failure controls on maximum sustainable overpressure in different tectonic stress regimes. Bull Am Assoc Petrol Geol 87:901–908
- Sminchak J, Gupta N (2003) Aspects of induced seismic activity and deep-well sequestration of carbon dioxide. Environ Geosci 10:81–89
- Soltanzadeh H, Hawkes CD (2009) Assessing fault reactivation tendency within and surrounding porous reservoirs during fluid production injection. Int J Rock Mech Min 46:1–7
- Spiers CJ, Liteanu E, Zhang X (2010) Compaction creep of granular calcite under upper crustal conditions. Effects of aqueous pore fluids and supercritical CO<sub>2</sub>. Geophysical research abstracts, 12, EGU2010-6816-1, EGU General Assembly 2010
- Stauffer PH, Viswanathan HS, Pawar RJ, Guthrie GD (2009) A system model for geologic sequestration of carbon dioxide. Environ Sci Technol 43:565–570
- Streit JE, Hillis RR (2004) Estimating fault stability and sustainable fluid pressures for underground storage of CO<sub>2</sub> in porous rock. Energy 29:1445–1456
- Taron J, Elsworth D, Min K-B (2009) Numerical simulation of thermal-hydrologic-mechanical-chemical processes in deformable fractured porous media. Int J Rock Mech Min Sci 46:842–854
- Tau Q, Ceckai D, Huertas N, Bryant SL (2011) An improved model to forecast CO<sub>2</sub> leakage rates along a wellbore. Energy Procedia 4:5385–5391

- Teatinia P, Gambolati G, Ferronato M, Settari A, Walters D (2011) Land uplift due to subsurface fluid injection. *J Geodyn* 51:1–16
- Ross GD, Todd, AC, Tweedie JA, Will AGS (1982) The dissolution effects of CO<sub>2</sub>-brine systems on the permeability of U.K. and North Sea calcareous sandstones. Society of petroleum engineers, SPE 10685-MS, SPE enhanced oil recovery symposium, 4–7 April 1982, Tulsa, Oklahoma
- Tran D, Nghiem L, Shrivastava V, Kohse B (2010) Study of geomechanical effects in deep aquifer CO<sub>2</sub> storage. In: Proceedings 44th US Rock mechanics symposium, Salt Lake City, Utah, USA, June 27–June 30, 2010
- Tsang C-F, Birkholzer J, Rutqvist J (2008) A comparative review of hydrologic issues involved in geologic storage of CO<sub>2</sub> and injection disposal of liquid waste. *Environ Geol* 54:1723–1737
- USEPA (U.S. Environmental Protection Agency) (1994) Determination of maximum injection pressure for class I wells, United States environmental protection agency region 5—underground injection control section regional guidance #7. EPA, Washington, DC
- Vasco DW, Ferretti A, Novali F (2008a) Estimating permeability from quasi-static deformation: temporal variations and arrival time inversion. *Geophysics* 73(6):O37–O52
- Vasco DW, Ferretti A, Novali F (2008b) Reservoir monitoring and characterization using satellite geodetic data: interferometric synthetic aperture radar observations from the Krechba field, Algeria. *Geophysics* 73(6):WA113–WA122
- Vasco DW, Rucci A, Ferretti A, Novali F, Bisell R, Ringrose P, Mathieson A, Wright I (2010) Satellite-based measurements of surface deformation reveal fluid flow associated with the geological storage. *Geophys Res Lett* 37:L03303
- Verdon JP, Kendall JM, Maxwell SC (2010) A comparison of passive seismic monitoring of fracture stimulation due to water versus CO<sub>2</sub> injection. *Geophysics* 75:MA1–MA7
- Verdon JP, Kendall JM, White DJ, Angus DA (2011) Linking microseismic event observations with geomechanical models to minimize the risks of storing CO<sub>2</sub> in geological formations. *Earth Planet Sci Lett* 305:143–152
- Vidal-Gilbert S, Nauroy J-F, Brosse E (2009) 3D geomechanical modelling for CO<sub>2</sub> geologic storage in the Dogger carbonates of the Paris Basin. *Int J Greenh Gas Control* 3: 288–299
- Vidal-Gilbert S, Tenthoirey E, Dewhurst D, Ennis-King J, Van Ruth P, Hillis R (2010) Geomechanical analysis of the Naylor Field, Otway Basin, Australia: implications for CO<sub>2</sub> injection and storage. *Int J Greenh Gas Control* 4:827–839
- Viegas G, Abercrombie RE, Kim W-Y (2010) The 2002 M5 Au Sable Forks, NY, earthquake sequence: source scaling relationships and energy budget. *J Geophys Res* 115: B07310
- Vilarrasa V, Bolster D, Olivella S, Carrera J (2010) Coupled hydromechanical modeling of CO<sub>2</sub> sequestration in deep saline aquifers. *Int J Greenh Gas Control* 4:910–919
- Wang W, Kolditz O (2007) Object-oriented finite element analysis of thermo-hydro-mechanical (THM) problems in porous media. *Int J Numer Methods Eng* 69:162–201
- White D (2009) Monitoring CO<sub>2</sub> storage during EOR at the Weyburn-Midale field. *Lead Edge* 28:838–842
- Wigand M, Kaszuba JP, Carey JW, Hollis WK (2009) Geochemical effects of CO<sub>2</sub> sequestration on fractured wellbore cement at the cement/caprock interface. *Chem Geol* 265:122–133
- Wright I (2011) In Salah CO<sub>2</sub> storage JIP lessons learned. 10th annual conference on carbon capture and sequestration, Pittsburgh, Pennsylvania, May 2–5, 2011
- Wright I, Ringrose P, Mathieson A, Eiken O (2009) An overview of active large-scale CO<sub>2</sub> storage projects. Society of petroleum engineers, SPE 127096, SPE international conference on CO<sub>2</sub> capture, storage, and utilization, 2–4 November 2009, San Diego, California, USA
- Yamamoto K, Takahashi K (2004) Importance of the geomechanics for the safety of CO<sub>2</sub> geologic sequestration. In: Proceedings of 3rd Asian Rock mechanics symposium, Nov 30–Dec 2, 2004, Kyoto, Japan
- Zhou Q, Birkholzer JT, Tsang C-F, Rutqvist J (2008) A method for quick assessment of CO<sub>2</sub> storage capacity in closed and semi-closed saline formations. *Int J Greenh Gas Control* 2:626–639
- Zhou R, Huang L, Rutledge J (2010) Microseismic event location for monitoring CO<sub>2</sub> injection using double-difference tomography. *Lead Edge* 29:201–214
- Zoback MD (2007) Reservoir geomechanics. Cambridge University Press, Cambridge
- Zoback MD (2010) The potential for triggered seismicity associated with geologic sequestration of CO<sub>2</sub> in saline aquifers. American Geophysical Union (AGU), EOS Trans. AGU, 91(52), Fall Meeting, Suppl., Abstract NH11C-01
- Zoback MD, Harjes HP (1997) Injection-induced earthquakes and crustal stress at 9 km depth at the KTB deep drilling site, Germany. *J Geophys Res Solid Earth* 102:18477–18491
- Zoback MD, Zinke JC (2002) Production-induced normal faulting in the Valhall and Ekofisk oil fields. *Pure Appl Geophys* 159:403–420
- Zoback MD, Zoback ML (1989) Tectonic stress field of the conterminous United States. *Geol Soc Am Mem* 172: 523–539